Editors' Suggestion

Free energy and specific heat near a quantum critical point of a metal

Shang-Shun Zhang [1], Erez Berg, [2] and Andrey V. Chubukov [1]
[1] School of Physics and Astronomy and William I. Fine Theoretical Physics Institute, University of Minnesota, Minneapolis, Minnesota 55455, USA
[2] Department of Condensed Matter Physics, Weizmann Institute of Sciences, Rehovot 76100, Israel

(Received 3 January 2023; revised 28 March 2023; accepted 30 March 2023; published 17 April 2023)

We analyze the free energy and the specific heat for fermions interacting with a gapless boson at a quantum-critical point (QCP) in a metal. We use the Luttinger-Ward-Eliashberg formula for the free energy in the normal state, which includes contributions from bosons, fermions, and their interaction, all expressed via fully dressed fermionic and bosonic propagators. The sum of the last two contributions is the free energy F_γ of an effective low-energy model of fermions with boson-mediated dynamical 4-fermion interaction $V(\Omega_m) \propto 1/|\Omega_m|^\gamma$ (the γ model). This purely electronic model has been used to analyze the interplay between non-Fermi liquid behavior and pairing near a QCP, which are both independent of the upper energy cutoff Λ. However, the specific heat $C_\gamma(T)$, obtained from F_γ, does depend on Λ. We argue that this dependence is spurious and cancels out, once we include the contribution from bosons. We further argue that the full $C(T)$ is the sum of the contribution from free fermions and the one from a critical boson, with the fully dressed propagator, other terms cancel out. We compare the full $C(T)$ with the $C_\gamma(T)$, obtained using recently proposed regularization of F_γ [Phys. Rev. B **106**, 054518 (2022)]. We argue that for $\gamma < 1$, the full $C(T)$ and the regularized $C_\gamma(T)$ differ by a γ-dependent prefactor, while for $\gamma > 1$, the full $C(T)$ and $C_\gamma(T)$ differ by the positive contribution from free massless fermions (a positive constant for the electron-phonon case $\gamma = 2$). For these γ, $C_\gamma(T)$ is negative, but the full $C(T)$ is positive. We argue that only the full $C(T)$ matters as the positive and the negative contributions originate from the term in $C(T)$ which contains the fully dressed bosonic propagator. We then argue that the normal state remains stable until the pairing instability develops.

DOI: 10.1103/PhysRevB.107.144507

I. INTRODUCTION

In this work we analyze in detail the free energy and specific heat of a metal near a critical point toward a spontaneous particle-hole order (Ising-nematic, antiferromagnetic, etc.), and of an electron-phonon system at vanishing dressed Debye frequency of an optical phonon. In all these cases, the low-energy physics is described by a model of fermions with Luttinger Fermi surface, coupled by Yukawa-type interaction to a near-massless boson, which represents either a critical fluctuation of a particle-hole order parameter or a soft optical phonon [1–21]. The key motivation for our study is current interest in a non-Fermi liquid (non-FL) behavior near a quantum-critical point (QCP). Numerous previous studies have shown [13–20,22–38] that at a QCP the self-energy at $T = 0$ is singular in the frequency domain and scales as $\Sigma(\omega) \propto \omega^{1-\gamma}$, where the exponent $\gamma \ll 1$ in weakly anisotropic 3D systems, $\gamma = 1/3$ at an Ising-nematic and Ising-ferromagnetic QCP in 2D, $\gamma \approx 1/2$ at a 2D QCP toward spin or charge density-wave order with a finite momentum, and $\gamma = 2$ for an electron-phonon problem. It is tempting to associate $1 + d\Sigma/d\omega$ with m^*/m and associate ω with T. By this reasoning, the leading term in the specific heat at small T, $C(T) \propto (m^*/m)T$, should scale as $T^{1-\gamma}$, i.e., as $T^{2/3}$ at an Ising-nematic QCP, as $T^{1/2}$ at a density-wave QCP, and as $1/T$ for critical electron-phonon problem (although this last behavior obviously cannot extend to $T = 0$). Our goal is to check whether these formulas hold in microscopic calculations.

A more specific motivation for our work is to clarify recent studies of the free energy for critical fermion-boson systems [38–43]. Some of us and others recently analyzed [37] the interplay between non-FL in the normal state and superconductivity within an effective low-energy model of fermions with boson-mediated dynamical 4-fermion interaction $V(\Omega) \propto 1/|\Omega|^\gamma$ (the γ model [44]). This model describes non-FL in the normal state and superconductivity. Both are universal phenomena in the sense that they come from fermions with energies well below the upper energy cutoff of the model Λ. The condensation energy—the difference between the free energy of a superconductor and of a would be normal state at the same T, is also independent on Λ [37]. However, the free energy of the γ model in the normal state is nonuniversal, even if we subtract its value at $T = 0$. Namely, its leading T-dependent term scales as $\Lambda T^{1-\gamma}$ [38]. The corresponding specific heat is then $C(T) \propto \Lambda/T^\gamma$, in variation with the estimate based on the self-energy. The authors of Refs. [41,42] argued that the dependence of the free energy and the specific heat on Λ is spurious and has to be regularized by adding the counter term to the free energy [41,42], which cancels out Λ dependence. Once this is done, the regularized specific heat becomes independent on Λ and scales as $T^{1-\gamma}$, as expected based on the self-energy. However, the regularization comes with the cost: the prefactor in $C(T) \propto T^{1-\gamma}$ turns out to be negative for $\gamma \geqslant 1$.[1]

Taken at a face value, a negative $C(T)$ would imply that the system becomes unstable below a certain T_{cr}, when a negative $T^{1-\gamma}$ term, coming from fermion-boson interaction, exceeds a positive $O(T)$ contribution to $C(T)$ from free fermions. A potential resolution would be that this instability is preempted by superconductivity, but it turns out that $T_{cr} > T_c$ [38,41,42] for γ larger than a certain critical value.

In this work, we analyze free energy and specific heat within the full fermion-boson model using the Luttinger-Ward-Eliashberg formula [45,46] for the variational free energy in the normal state. We assume that superconductivity is suppressed, and extend the normal state analysis down to small T. Luttinger and Ward argued [45] that the free energy of a system of fermions with 4-fermion interaction can be expressed diagrammatically by collecting compact skeleton diagrams with fully dressed fermionic propagators and using conventional rules of the diagrammatic technique, but one has to add to free energy the term F_{el}, which explicitly contains fermionic self-energy Σ (see below). This additional term is constructed such that the stationary condition $\delta F/\delta\Sigma = 0$ reproduces the diagrammatic series for the self-energy. Eliashberg extended Luttinger-Ward approach to the case of electron-phonon interaction. He argued that the free energy for such a system is obtained by collecting compact skeleton diagrams with fully dressed fermionic and bosonic propagators, and contains the second extra term F_{bos}, which depends on the bosonic polarization operator Π (the bosonic self-energy) and is constructed such that the stationary condition $\delta F/\delta\Pi = 0$ reproduces diagrammatic series for Π.

We analyze the electron-phonon model and different electronic models in which a certain collective bosonic mode becomes massless at a QCP. For these models, the low-energy behavior of fermions and their soft collective excitations is captured within an effective fermion-boson model, in which a collective mode becomes an independent degree of freedom, coupled to fermions.

The full variational free energy of fermion-boson model is $F = F_{\text{bos}} + F_{\text{el}} + F_{\text{int}}$, where F_{int} is the sum of skeleton diagrams. We assume, following earlier works, that both phonons and soft collective modes are slow compared to dressed fermions, either because a velocity of a boson is small compared to that of a dressed fermion, or because collective bosons are Landau overdamped, and that the smallness of an (effective) velocity of a boson is controlled by a dimensionless parameter λ_E, often called Migdal-Eliashberg parameter (more on this below). In practical terms, the fact that the bosons are slow compared to fermions means that corrections to fermion-boson vertex are small as in the processes identified with vertex corrections fermions are forced to vibrate at boson frequencies, far away from their own resonance. This makes higher-loop terms in the skeleton loop expansion of F_{int} small compared to the one-loop term, and we keep only this term in F_{int} (see Sec. III B for more details).

[1]The authors of Refs. [41,42] found the prefactor to be negative for $\gamma \geqslant 2$, which they only considered. The authors of Refs. [38] argued that the prefactor is negative for $\gamma > 1$.

The free energy of the γ-model is $F_\gamma = F_{\text{el}} + F_{\text{int}}$. Like we said, the specific heat obtained from F_γ depends on the cutoff. Our goal is to understand the role of F_{bos}, specifically (i) whether it acts as the counter term, which eliminates the cutoff dependence of F_γ, and (ii) whether it also affects the universal part of $C(T)$.

We show below that for any γ, the full free energy F near a QCP is

$$F = -2\pi T N_F \sum_m |\omega_m| + \frac{T}{2}\sum_q \log\left[-D_q^{-1}\right], \tag{1}$$

where the first term is the contribution from free fermions, and in the second D_q is the fully dressed bosonic propagator $[q \equiv (\mathbf{q}, \Omega_m),\ \Omega_m = 2\pi T m]$. This result holds even if we include thermal fermionic self-energy, which near a QCP we compute self-consistently, extending beyond the Eliashberg theory [29]. The bosonic propagator D_q contains information about fermion-boson interaction as it contains the bosonic polarization bubble. We compute the specific heat from Eq. (1), compare it with the one of the regularized γ model, and address the issues (i) and (ii). Regarding (i), we find that F_{bos} cancels the cutoff-dependent terms in F_γ, i.e., it provides the physical realization of the counter term suggested in Refs. [41,42]. On (ii), the result depends on whether $\gamma < 1$ or $\gamma > 1$. For $\gamma < 1$ (Ising-nematic and related models), the contribution to the specific heat from F_{bos} is of the same order as the one from the regularized F_γ. The two contributions differ by a γ-dependent factor. For the values of the exponent $\gamma > 1$, which include the electron-phonon case ($\gamma = 2$), the contribution from F_{bos} to $C(T)$ coincides with that from free bosons (a T-independent term for $\gamma = 2$). The full F in this case [Eq. (1)] is the sum of the contributions from a free boson and from the regularized γ model. The last contribution is negative at small T, in agreement with Refs. [41,42]. However, the negative term appears in Eq. (1) as the subleading term in the expansion $\log[-D_q^{-1}]$ to first order in the dynamical bosonic polarization, while the positive contribution from a free boson is the leading term. The expansion holds in powers of the Migdal-Eliashberg parameter λ_E (defined below), and we argue that as long as $\lambda_E \leqslant 1$, i.e., as long as the theory is under control, the specific heat is positive. Based on this, we argue that the normal state remains stable near a QCP, until (and if) a pairing instability develops. In this last respect our conclusions are different from those in Refs. [41,42].

The structure of the paper is as follows. In Sec. II we present the generic Luttinger-Ward-Eliashberg expression for the free energy, briefly discuss the Eliashberg theory, and use it to obtain the expressions for the full F, Eq. (1), and for F_γ in the purely fermionic γ model. In Sec. III we compare the two expressions for the Ising-nematic model in 2D. Here we also show that the result for F does not change if we include thermal self-energy, which has to be calculated outside the Eliashberg theory, and estimate the strength of vertex corrections once we include thermal self-energy. We also discuss the role played by the thermal mass of a boson. In Sec. IV we consider antiferromagnetic QCP in 2D. In Sec. V we consider an electron-phonon system near a QCP. Here we also discuss, in Sec. V A, the regularization of F_γ from physical perspective. In Sec. VI we extend the $\gamma = 2$ model to arbitrary

γ between 1 and 2 and compute the specific heat. We show that the full specific heat is positive, as long as $\lambda_E \leqslant 1$, despite that the contribution from the regularized F_γ is negative. We present our conclusions in Sec. VII. Some technical details of the calculations are presented in the Appendices.

II. FREE ENERGY AND SPECIFIC HEAT

The variational free energy for interacting fermions has been derived by Luttinger and Ward [45] and extended to fermion-boson systems by Eliashberg [46] (see also Refs. [47,48]). For more recent studies of variational free energy, see Refs. [38–40,49–52]. The free energy per unit volume is the sum of the fermionic contribution, the bosonic contribution, and the contribution due to fermion-boson interaction:

$$F = F_{\rm el} + F_{\rm bos} + F_{\rm int}. \tag{2}$$

The fermionic part is

$$F_{\rm el} = -2T\sum_k \log G_k^{-1} + 2iT\sum_k \Sigma_k G_k, \tag{3}$$

where $k \equiv (\mathbf{k}, \omega_m)$, $\omega_m = \pi T(2m+1)$, $T\sum_k = T\sum_m \int d\mathbf{k}/(2\pi)^d$ (d is the spatial dimension), $\tilde{\Sigma}_k = \omega_m + \Sigma_k$, where Σ_k is the self-energy, and $G_k = (i\tilde{\Sigma}_k - \epsilon_{\mathbf{k}})^{-1}$ is the Green's function.

The bosonic part is

$$F_{\rm bos} = \frac{T}{2}\sum_q \left(\log\left[-D_q^{-1}\right] + \Pi_q D_q\right), \tag{4}$$

where $q \equiv (\mathbf{q}, \Omega_m)$, $\Omega_m = 2\pi T m$, Π_q is the bosonic self-energy, and $D_q = [(D_q^0)^{-1} - \Pi_q]^{-1}$ is the dressed bosonic propagator. For the bare bosonic propagator we set $D_q^0 = -D_0/(\Omega_m^2 + \omega_D^2)$ for the electron-phonon case, where ω_D is a bare Debye frequency, $D_q^0 = -D_0/[(\Omega_m/c)^2 + \boldsymbol{q}^2 + m_{i-n}^2]$ for the Ising-nematic case, and $D_q^0 = -D_0/[(\Omega_m/c)^2 + (\boldsymbol{q} - \boldsymbol{Q})^2 + m_{\rm afm}^2]$ for the antiferromagnetic case, where $\boldsymbol{Q} = (\pi, \pi)$, and c is of order of Fermi velocity v_F. We set the lattice constant $a = 1$. For the last two cases, the Ω_m^2 term in the bosonic propagator can be neglected as for relevant Ω_m it is parametrically smaller than the Landau damping term from Π_q. On the contrary, for the electron-phonon case, Ω_m^2 term is more relevant than the Landau damping.

Finally, the interaction part is

$$F_{\rm int} = -T^2\sum_{k,k'} g^2_{|\mathbf{k}-\mathbf{k}'|} G_k D(k-k') G_{k'} + \cdots, \tag{5}$$

where $g_{\boldsymbol{q}}$ is the Yukawa coupling. The dots in Eq. (5) stand for higher-order contributions, which account for vertex corrections (see Ref. [50,53] for the discussion on higher-order terms in the loop expansion of $F_{\rm int}$). We assume, following Ref. [46], that vertex corrections can be neglected (more on this below). For simplicity, we also approximate $g_{\boldsymbol{q}}$ by g. We refer to the free energy described by Eqs. (2)–(5) as the Eliashberg free energy.

The stationary solutions for Σ_k and Π_k are obtained from $\delta F/\delta\Sigma_k = 0$ and $\delta F/\delta\Pi_q = 0$. They give rise to two Eliashberg equations for fermionic and bosonic self-energies [39,40,45,46,49,50,53] (see Fig. 1)

$$\Sigma_k = -iT\sum_q g^2 G_{k-q} D_q, \tag{6}$$

$$\Pi_q = 2g^2 T\sum_k G_k G_{k-q}, \tag{7}$$

where the factor 2 in Eq. (7) accounts for the spin degeneracy. These equations are the same as one obtains diagrammatically, without invoking the free energy. We emphasize in this regard that the diagrammatic loop expansion with full G and full D holds only for $F_{\rm int}$. The terms $F_{\rm el}$ and $F_{\rm bos}$ are additional contributions to the free energy, constructed to reproduce Eqs. (6) and (7) as stationary conditions for the full F.

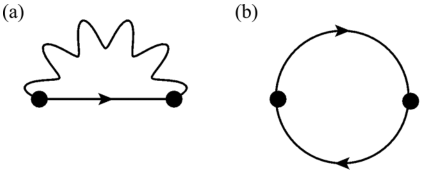

FIG. 1. Self-energy of (a) electron $i\Sigma(k)$ and (b) boson $-\Pi(q)$ (the polarization bubble). The solid (waggle) lines denote the dressed electron (boson) Green's functions. The polarization bubble contains factor of 2 from the spin degeneracy.

Below we will analyze the free energy in equilibrium, when Σ_k and Π_q obey Eqs. (6) and (7). One can easily check that in this situation

$$T/2\sum_q \Pi_q D_q = iT\sum_k \Sigma_k G_k, \tag{8}$$

because both expressions describe the same skeleton diagram; see Fig. 2. Along the same lines,

$$F_{\rm int} = -iT\sum_k \Sigma_k G_k. \tag{9}$$

Using these two expressions, we obtain

$$F = -2T\sum_k \log G_k^{-1} + 2iT\sum_k \Sigma_k G_k + \frac{T}{2}\sum_q \log\left[-D_q^{-1}\right], \tag{10}$$

and separately

$$F_{\rm el} + F_{\rm int} = -2T\sum_k \log G_k^{-1} + iT\sum_k \Sigma_k G_k. \tag{11}$$

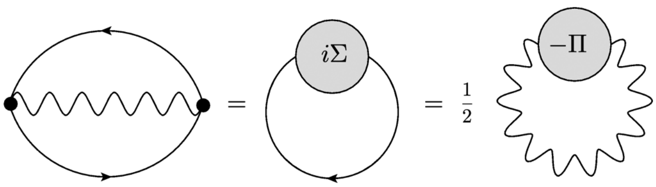

FIG. 2. Thermodynamic potential due to fermion-boson interaction. The three diagrams are equivalent if we substitute the self-energy Σ and the polarization Π in Eqs. (6) and (7).

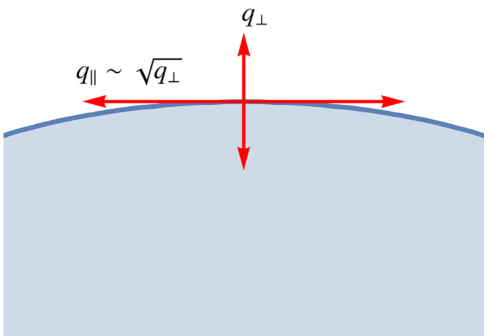

FIG. 3. Typical transverse and longitudinal momenta, $q_\perp$ and $q_\parallel$, for the Ising-nematic case. At small $\mathbf{q}$, $q_\parallel \gg q_\perp$.

A. Eliashberg theory

The Eliashberg formula for the free energy is valid when bosons are slow compared to the fermions, either because $\omega_D \ll E_F$ in the electron-phonon problem or because the collective boson is Landau overdamped. An extension to $N \gg 1$ fermionic flavors, which individually interact with a boson, enhances the magnitude of the Landau damping term and increases the applicability range of the Eliashberg theory [3,4,13,17,19,54–56].

The condition that the bosons are slow compared to the fermions allows one to factorize the momentum integration along and transverse to the Fermi surface because in all three cases that we consider, the typical transverse momenta are much smaller than typical longitudinal momenta (we illustrate this in Fig. 3). To obtain the leading contribution to the right-hand side (r.h.s.) of Eq. (6) one can then integrate over transverse $q_\perp$ in the fermionic propagator and over $q_\parallel$ in the bosonic propagator with $\mathbf{q}$ connecting points on the Fermi surface [49]. Integrating over momenta this way and extending both integrations to infinity [57], one obtains a purely dynamical self-energy

$$\Sigma_k = \Sigma(\omega_n) = \pi T \sum_m \text{sgn}(\omega_n + \Omega_m) D_{\text{loc}}(\Omega_m). \tag{12}$$

At $T = 0$,

$$\Sigma(\omega_n) = \int_0^{\omega_n} D_{\text{loc}}(\Omega_m) d\Omega_m. \tag{13}$$

The form of D_{loc} is model-specific, but in all cases we have at a QCP

$$D_{\text{loc}}(\Omega_m) = \left(\frac{\bar{g}}{|\Omega_m|} \right)^\gamma, \tag{14}$$

where $\gamma = 1/3$ for the Ising-nematic case, $\gamma = 1/2$ for the antiferromagnetic case, and $\gamma = 2$ for the electron-phonon case. The coupling $\bar{g}$ is expressed via g (see Secs. III, IV, and V). Away from the QCP, Eq. (14) is modified to

$$D_{\text{loc}}(\Omega_m) = \left(\frac{\bar{g}^2}{\Omega_m^2 + M^2} \right)^{\gamma/2}, \tag{15}$$

where $M \sim m_{\text{i-n}}^3$ for Ising-nematic case, $M \sim m_{\text{afm}}^2$ for antiferromagnetic case, and $M = \bar{\omega}_D$ (the renormalized Debye frequency) for the electron-phonon case. We assume that M and ω_D do not depend on temperature, or, more accurately, that their temperature dependence does not modify $C(T)$ to the leading order in T compared to what we find below. We verify this by comparing our $C(T)$ with the contribution from $M(T)$ from mode-mode coupling, introduced in Hertz-Millis-Moriya theory [58].

Because Σ_k in Eq. (12) does not depend on $\epsilon_{\boldsymbol{k}}$, one can explicitly integrate over momentum in Eq. (3) using $\int d^d k/(2\pi)^d = N_F \int d\epsilon_{\boldsymbol{k}}$, where N_F is the density of states at the Fermi level per spin component. The integration yields

$$-2T \sum_k \log G_k^{-1} = -2\pi T N_F \sum_m (|\omega_m| + |\Sigma(\omega_m)|),$$
$$2iT \sum_k \Sigma_k G_k = 2\pi T N_F \sum_m |\Sigma(\omega_m)|. \tag{16}$$

Combing the two contributions, we find that the self-energy cancels out and F_{el} retains the same as for free fermions:

$$F_{\text{el}} = -2\pi T N_F \sum_m |\omega_m|. \tag{17}$$

We emphasize that this holds only if Σ_k does not depend on $\epsilon_{\boldsymbol{k}}$ (see Appendix B for an extended discussion). For a generic momentum and frequency dependent Σ_k, F_{el} does depend on the fermionic self-energy.

Applying the same procedure to Eqs. (10) and (11) we obtain [38,40,49,50]

$$F = -2\pi T \sum_m |\omega_m| + \frac{T}{2} \sum_q \log\left[-D_q^{-1}\right]$$
$$= F_{\text{free}} + \frac{T}{2} \sum_q \log\left[-D_q^{-1}\right] \tag{18}$$

and

$$F_{\text{el}} + F_{\text{int}} = -2\pi T N_F \sum_m |\omega_m| - \pi T N_F \sum_m |\Sigma(\omega_m)|. \tag{19}$$

Note that the self-energy $\Sigma(\omega_m)$ cancels out in F, and that the dependence on fermion-boson interaction comes about because D_q depends on the polarization $\Pi(q)$.

At $T = 0$, $\Sigma(\omega_m) = [\bar{g}^\gamma/(1-\gamma)]|\omega_m|^{1-\gamma}\text{sgn}\omega_m \equiv \omega_0^\gamma |\omega_m|^{1-\gamma}\text{sgn}\omega_m$, where $\omega_0 = \bar{g}/(1-\gamma)^{1/\gamma}$. This holds for $\gamma < 1$. For $\gamma > 1$, one has to add the contribution from the lower limit in Eq. (13). This last contribution scales as $1/M^{\gamma-1}$ and diverges at $M \to 0$. However, it does not contribute to the specific heat, as one can explicitly verify. At a finite T, the self-energy becomes a function of a Matsubara number, and there appears a separate singular contribution $O(1/M^\gamma)$ from zero bosonic Matsubara frequency. This last contribution requires special attention, and we discuss it in some detail in Sec. III.

B. A purely electronic γ model

The γ model is designated to reproduce some low-energy properties of the fermion-boson system (more specifically, non-FL and superconductivity). It is a fermion-only model in which $D_{\text{loc}}(\Omega_m)$ from Eq. (15) plays the role of an effective dynamical 4-fermion interaction [37]. The model allows one to analyze the interplay between non-FL and pairing by solving coupled Eliashberg equations for the dynamic fermionic self-energy and the dynamic pairing vertex $\Phi(\omega_m)$. In a more common and convenient formulation, these equations are re-expressed in terms of the superconducting gap function $\Delta(\omega_m)$ and the inverse quasiparticle residue $Z(\omega_m)$. By construction, the model contains only the fermions, and its free energy in the normal state is $F_\gamma = F_{\rm el} + F_{\rm int}$, given by Eq. (19),

$$F_\gamma = -2\pi T N_F \sum_m |\omega_m| - \pi^2 T^2 N_F \bar{g}^\gamma \times \sum_{m,m'} \frac{\text{sgn}(\omega_m \omega_{m'})}{[(\omega_m - \omega_{m'})^2 + M^2]^{\gamma/2}}. \tag{20}$$

The summation over m is confined to frequencies below the upper energy cutoff Λ of the γ-model. In practice, this implies that the summation holds over M_f positive and M_f negative fermionic Matsubara frequencies $\omega_n = \pi T(2n+1)$ ($-M_f < n < M_f - 1$). The relation between M_f and Λ can be obtained by comparing the exact sum of $|\omega_m|$ with Euler-Maclauren formula, in which the integral is cut by Λ. The comparison yields [38] $4\pi^2 T^2 M_f^2 = \Lambda^2 + \pi^2 T^2/3$, hence

$$M_f = \tilde{\Lambda}\left(1 + \frac{1}{24\tilde{\Lambda}^2} + \cdots\right), \tag{21}$$

where $\tilde{\Lambda} = \Lambda/(2\pi T)$.

Applying this procedure to both terms in Eq. (20), we obtain [38] at $T \gg M$

$$\begin{aligned} F_\gamma = &-N_F\left[\Lambda^2 - \bar{g}^\gamma \Lambda^{2-\gamma}\frac{2(1-2^{-\gamma})}{(1-\gamma)(2-\gamma)}\right] \\ &- N_F \pi T \Lambda \left(\frac{\bar{g}}{M}\right)^\gamma - N_F \Lambda \bar{g}^\gamma (2\pi T)^{1-\gamma}\zeta(\gamma) \\ &+ N_F\left[\frac{3}{2}\bar{g}^\gamma (2\pi T)^{2-\gamma}\zeta(\gamma-1) - \frac{1}{3}\pi^2 T^2\right], \end{aligned} \tag{22}$$

where $\zeta(s)$ is the Riemann ζ function. The first two terms in Eq. (22) constitute the free energy at $T = 0$. The next one, with M in the denominator, comes from the thermal piece in $\Sigma(\omega_m)$ in Eq. (19), or, equivalently, from the $m = m'$ term in Eq. (20). The next term comes from $\omega_m, \omega_{m'} \sim \Lambda$, but $\omega_m - \omega_{m'} = O(T)$. The last term is the combination of cutoff independent contributions from both terms in Eq. (20).

The specific heat $C_\gamma(T) = -T d^2 F_\gamma / d^2 T$ is

$$\begin{aligned} C_\gamma(T) = &\, 2\pi \Lambda N_F \left(\frac{\bar{g}}{2\pi T}\right)^\gamma \gamma(\gamma-1)\zeta(\gamma) \\ &+ \frac{2}{3}\pi N_F\left[\pi T - \frac{9}{4}\bar{g}^\gamma (2\pi T)^{1-\gamma}(\gamma-2) \right. \\ &\left. \times (\gamma-1)\zeta(\gamma-1)\right]. \end{aligned} \tag{23}$$

The first term in Eq. (23) is parametrically larger than the other two since it is proportional to Λ. This term is positive, but depends linearly on the upper energy cutoff. The second term is a universal contribution to $C(T)$. This term is positive for $\gamma < 1$, but becomes negative at small $T < T_0 = [\bar{g}/(2\pi)][9(\gamma-2)(\gamma-1)\zeta(\gamma-1)/2]^{1/\gamma}$ for $\gamma > 1$, when $(\gamma-2)(\gamma-1)\zeta(\gamma-1) > 0$. The temperature T_0 increases with γ up to $\gamma = 3$.

The authors of Refs. [40–42] argued that the dependence of $C(T)$ on the cutoff is spurious and must be eliminated by a proper regularization. They suggested that this is achieved by adding to the r.h.s. of Eq. (20) the term

$$\pi^2 T^2 N_F \bar{g}^\gamma \sum_{m,m'} \frac{1}{[(\omega_m - \omega_{m'})^2 + M^2]^{\gamma/2}}. \tag{24}$$

This additional term cancels out all Λ-dependent terms in F_γ in Eq. (22) and changes the prefactor for the universal $T^{2-\gamma}$ term. The regularized free energy, which we label as $\bar{F}_\gamma$, is

$$\bar{F}_\gamma = N_F\left[\bar{g}^\gamma (2\pi T)^{2-\gamma}\zeta(\gamma-1) - \tfrac{1}{3}\pi^2 T^2\right]. \tag{25}$$

This yields a universal, cutoff-independent specific heat $\bar{C}_\gamma(T)$. At a QCP,

$$\bar{C}_\gamma(T) = 2\pi N_F\left[\frac{\pi}{3}T - \bar{g}^\gamma (2\pi T)^{1-\gamma}(\gamma-2) \times (\gamma-1)\zeta(\gamma-1)\right]. \tag{26}$$

For $\gamma < 1$, all terms in Eq. (26) are positive as $\zeta(\gamma-1)$ is negative. For $\gamma = 1/3$,

$$\bar{C}_{1/3}(T) = 2\pi N_F\left[\frac{\pi}{3}T + 0.172\bar{g}^{1/3}(2\pi T)^{2/3}\right]. \tag{27}$$

For $\gamma > 1$, $C(T)$ given by Eq. (26) is still negative at small T because $(\gamma-2)(\gamma-1)\zeta(\gamma-1) > 0$. For $\gamma \to 2$,

$$\bar{C}_2(T) = 2\pi N_F\left(\frac{\pi}{3}T - \frac{\bar{g}^2}{2\pi T}\right). \tag{28}$$

C. Underlying fermion-boson model

We now return back to the underlying fermion-boson model, in which there is an additional bosonic contribution to the free energy, and check whether the effect of $F_{\rm bos}$ is the same as of the extra term (24), which regularizes F_γ.

The full free energy $F = F_{\rm el} + F_{\rm bos} + F_{\rm int} = F_\gamma + F_{\rm bos}$ is given by Eq. (18) as the sum of the free-fermion contribution and the one expressed via the full bosonic propagator. In contrast, F_γ, given by Eq. (19), depends explicitly on the fermionic self-energy. Below we study the relation between these two expressions. We show that the outcome depends on the type of a QCP. To see this, we consider separately Ising-nematic QCP, antiferromagnetic QCP, and a QCP of an electron-phonon system.

III. ISING-NEMATIC QCP

We consider a 2D system. The bare bosonic propagator has the Ornstein-Zernike form $D_q^0 = -D_0/(q^2 + m_{\rm i\text{-}n}^2)$. The static part of $\Pi(q)$ renormalizes D_0 and m. We assume that these renormalizations are already incorporated into D_q^0. The dynamical part of $\Pi(q)$ accounts for the Landau damping: $\Pi(\mathbf{q}, \Omega_m) - \Pi(\mathbf{q}, 0) = (1/D_0)\alpha|\Omega_m|/|\mathbf{q}|$. For a circular Fermi surface, $\alpha = g^* k_F/(\pi v_F^2)$, where $g^* = g^2 D_0$ has the dimension of energy and plays the role of an effective fermion-boson interaction. The dressed bosonic propagator is

$$D_q = -\frac{D_0}{|\mathbf{q}|^2 + m_{\rm i\text{-}n}^2 + \alpha\frac{|\Omega_m|}{|\mathbf{q}|}}. \tag{29}$$

Integrating over one momentum component and comparing the result with $D_{\rm loc}(\Omega_m)$ from Eq. (14) for $\gamma = 1/3$, we obtain $\bar{g} = (g^*)^2/(162\sqrt{3}\pi^2 E_F)$ and $\omega_0 = (27/8)\bar{g} = (g^*)^2/(48\sqrt{3}\pi^2 E_F)$. The mass $m_{\text{i-n}}$ is related to M in the γ model by $M = 32\pi/(81\sqrt{3})(m_{\text{i-n}} v_F)^3/(g^* E_F)$.

Substituting D_q into Eq. (18), subtracting from $\log[-D_q^{-1}]$ its static part, which does not contribute to the specific heat, and integrating over momentum (the integral converges), we obtain at a QCP (i.e., at $m_{\text{i-n}} = 0$)

$$F = F_{I-N} = F_{\rm free} + \frac{\alpha^{2/3}}{4\pi\sqrt{3}}(2\pi T)^{5/3}\sum_1^{M_b} n^{2/3}$$
$$= F_{\rm free} + \frac{\alpha^{2/3}}{4\pi\sqrt{3}}(2\pi T)^{5/3} H_{-2/3}(M_b), \quad (30)$$

where $F_{\rm free} = -N_F(\Lambda^2 + \pi^2 T^2/3)$ is free energy of a gas of free fermions, M_b is the upper cutoff for summation over n, and $H_p(M_b) = \sum_1^{M_b} 1/k^p$ is the Harmonic number. The asymptotic expansion of $H_p(M_b)$ at large M_b is

$$H_p(M_b) = \frac{\left(M_b + \frac{1}{2}\right)^{1-p}}{1-p} + \zeta(p) + O\left(1/M_b^{p+1}\right). \quad (31)$$

The relation between M_b and the cutoff Λ can be established in a way similar to the procedure described above for fermions, by evaluating $\sum_{m=1}^{M_b} m$ directly and using Eular-Maclaurin formula with Λ as the upper cutoff of frequency integration. This yields

$$M_b + \frac{1}{2} = \tilde{\Lambda}\left(1 + \frac{1}{24\tilde{\Lambda}^2} + \cdots\right). \quad (32)$$

We remind that $\tilde{\Lambda} = \Lambda/(2\pi T)$. Substituting into Eq. (30), we obtain

$$F_{I-N} = -N_F\Lambda^2 + \frac{\sqrt{3}(\alpha A)^{2/3}}{20\pi}\Lambda^{5/3}$$
$$- \frac{\pi^2}{3}N_F T^2 + \frac{\alpha^{2/3}}{4\pi\sqrt{3}}(2\pi T)^{5/3}\zeta(-2/3), \quad (33)$$

where $\zeta(-2/3) \simeq -0.155$. Differentiating with respect to T, we find that both the entropy $S_{I-N}(T) = -dF_{I-N}/dT$ and the specific heat $C_{I-N}(T) = -T d^2F_{I-N}/dT^2 = (2/3)S_{I-N}(T)$ are independent on Λ. The specific heat is

$$C_{I-N}(T) = \frac{2\pi^2}{3}N_F T - \frac{5\alpha^{2/3}}{9\sqrt{3}}(2\pi T)^{2/3}\zeta(-2/3). \quad (34)$$

Re-expressing the result in terms of $\bar{g}$ from Eq. (14), we obtain

$$C_{I-N}(T) = \frac{2\pi^2}{3}N_F T - \frac{5}{3}\bar{g}^{1/3}(2\pi T)^{2/3}\zeta(-2/3). \quad (35)$$

Comparing this $C_{\text{I-N}}(T)$ with the $\tilde{C}_{1/3}(T)$ from Eq. (27) (a regularized specific heat in the γ model), we see that they agree up to a numeric prefactor in the $T^{2/3}$ term (the prefactor in $C_{\text{I-N}}(T)$ is larger by 3/2). The number 3/2 is the difference between the momentum integral of $\log(-D_q^{-1})$ with static term subtracted and the momentum integral of $\Pi_q D_q$, i.e., between $\int_0^\infty dxx\log(1 + 1/x^3) = \pi/\sqrt{3}$ and $\int_0^\infty dx/(x^3 + 1) = (2/3)(\pi/\sqrt{3})$.

The analysis at the Ising-nematic QCP can be formally extended to other values of γ if we replace q^2 in D_q by q^a with some $a > 1$. The exponent γ then changes from 1/3 to $\gamma = (a-1)/(a+1)$, which ranges between 0 and 1. One can easily verify (see Appendix D) that the interaction contributions to $C_{I-N}(T)$ in the Ising-nematic model and in the regularized γ-model have the same structure and just differ by $1-\gamma$ [the prefactor is larger in $C_{\text{I-N}}(T)$].

The conclusion here is that for the Ising-nematic case and its extensions, the functional form of the specific heat is reproduced if one restricts itself to the pure fermionic γ-model and either regularizes the free energy, as suggested in Refs. [40–42], or just eliminates the cutoff-dependent term in the specific heat in Eq. (23).

A. Distinction between quantum and thermal fluctuations

Equation (18) for the free energy is obtained under the assumption that the momentum dependence of the self-energy can be neglected for $\epsilon_{\boldsymbol k} \sim \tilde{\Sigma}(\omega)$. As we said above, this is the case when typical momenta transverse to the Fermi surface in Eq. (6) are much smaller than typical momenta along the Fermi surface for the same frequency, and one can factorize the momentum integration. At $T = 0$, this holds both at the QCP and away from it. At the QCP we have $q_\perp^{\rm typ} \sim \tilde{\Sigma}(\omega)/v_F$ and $q_\parallel^{\rm typ} \sim (\alpha\omega)^{1/3}$. We use $\tilde{\Sigma}(\omega) = \omega + \omega_0^{1/3}\omega^{2/3}$, where $\omega_0 \simeq (g^*)^2/E_F \sim \bar{g}$. A simple analysis shows that $q_\parallel^{\rm typ} \gg q_\perp^{\rm typ}$ up to $\omega_{\rm max} \sim (g^* E_F)^{1/2} \sim \bar{g}^{1/4}E_F^{3/4}$. This scale is much larger than the upper cutoff for non-FL behavior, $\omega_0 \sim \bar{g}$, which is also a typical scale for superconductivity. Away from a QCP, typical $q_\parallel^{\rm typ} \sim \max\{m, (\alpha\omega)^{1/3}\}$ are even larger. We note in passing that the factorization of the momentum integration eliminates the dependence on $\Sigma(\omega)$ in the r.h.s. of Eq. (6), i.e., the full Green's function in this equation can be safely replaced by the bare one.

At a finite T the self-energy Σ_k can be split into two parts [4,23,29,31,34]. One is the thermal part, $\Sigma_k^{\rm th}$, which comes from zero bosonic Matsubara frequency, and the other is the quantum part, Σ_k^q, which comes from the summation over all nonzero Matsubara frequencies. For the quantum part, taken alone, the condition $q_\parallel^{\rm typ} \gg q_\perp^{\rm typ}$ holds up to $\omega_{\rm max}$, and one can evaluate Σ^q using Eq. (12). For $T \gg M$,

$$\Sigma_k^q = {\rm sgn}(\omega_m)\left\{\tfrac{3}{2}\bar{g}^{1/3}|\omega_m|^{2/3}[1 + O(T/\omega_m)]\right.$$
$$\left. + \zeta(1/3)\bar{g}^{1/3}(2\pi T)^{2/3}\right\} \quad (36)$$

(see Ref. [29] for the analysis of Σ_k^q at all T).

For the thermal part, the situation is different: the condition $q_\parallel^{\rm typ} \gg q_\perp^{\rm typ}$ holds only away from a QCP, at a finite bosonic mass $m_{\text{i-n}} > \tilde{\Sigma}_k/v_F$, where $\tilde{\Sigma}_k = \omega + \Sigma_k^{\rm th} + \Sigma_k^q$. Under this condition, we obtain

$$\Sigma_k^{\rm th} = {\rm sgn}(\omega_m)\frac{g^* T}{4m_{\text{i-n}}v_F} = {\rm sgn}(\omega_m)\pi T\left(\frac{\bar{g}}{M}\right)^{1/3}. \quad (37)$$

A straightforward analysis shows that Eq. (37) is valid for $T < T^* \sim (m_{\text{i-n}}/k_F)^2 E_F^2/g^*$. At the QCP, T^* vanishes if we treat $m_{\text{i-n}}$ as temperature-independent. The thermal contribution to the self-energy then has to be computed differently, by integrating over both components of momenta in the fermionic

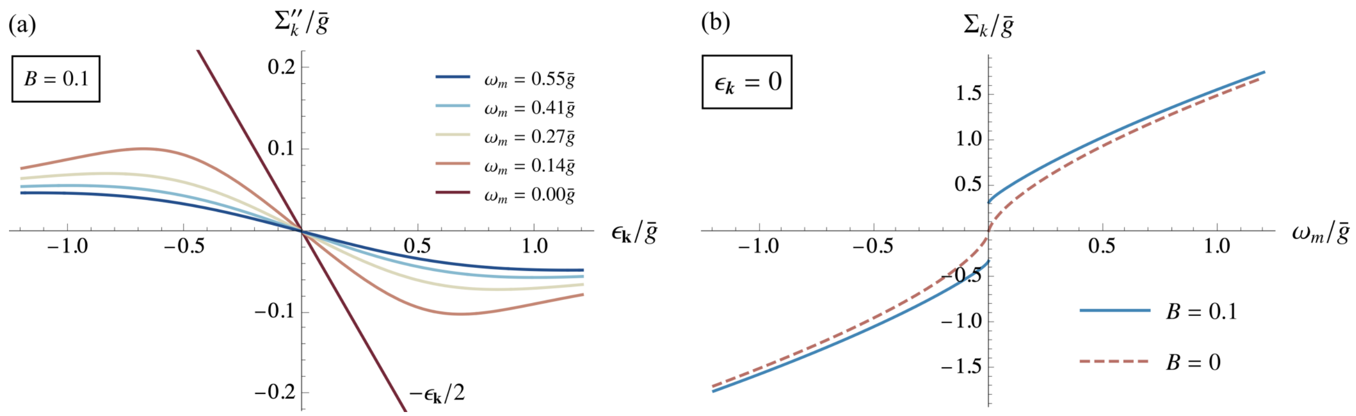

FIG. 4. (a) The imaginary part of Σ_k for different values of ω_m at $B = 0.1$. (b) $\Sigma_k \equiv \Sigma'_k$ at $\epsilon_{\mathbf{k}} = 0$ at $B = 0$ and $B = 0.1$ (dashed and solid lines, respectively).

propagator. For the one-loop self-energy this yields

$$\Sigma_k^{\text{th}} = iBG_k = \frac{B}{\tilde{\Sigma}_k + i\epsilon_k}, \tag{38}$$

where $B = g^* T \log(k_F/m_{\text{i-n}})$ and $\tilde{\Sigma}_k = \omega + \Sigma_k^q + \Sigma_k^{\text{th}} = \tilde{\Sigma}_k^q + \Sigma_k^{\text{th}}$.

Equation (38) shows that B and the thermal self-energy logarithmically diverge at a QCP, where $m_{\text{i-n}} = 0$. This divergence is an artifact of treating $m_{\text{i-n}}$ as T-independent. There are no T-dependent corrections to $m_{\text{i-n}}$ within the low-energy theory, but the bare $m_{\text{i-n}}$ generally possesses some T dependence coming from high-energy fermions. This T dependence leads to a variation of the Ising-nematic ordering temperature with the parameter that brings the system to the instability. Because the divergence in Eq. (38) is only logarithmic, it is cut in the same way by any T dependence of $m_{\text{i-n}}$. It has been argued [34,56,59], that, up to a prefactor, $\log(k_F/m_{\text{i-n}})$ can be approximated by $\log(E_F/T)$. We follow these works and just set $B = g^* T \log(E_F/T)$.

The key new feature of Σ_k^{th} from Eq. (38) is that it depends on both ω_m and $\epsilon_{\mathbf{k}}$. Then one has to redo the integration over $\epsilon_{\mathbf{k}}$ in the fermionic part of the free energy in Eq. (10). To do this, we solve Eq. (38) for Σ^{th} in terms of $\tilde{\Sigma}^q = \omega_m + \Sigma^q(\omega_m)$ and $\epsilon_{\mathbf{k}}$. We obtain

$$\Sigma_k^{\text{th}} = \sqrt{B + \left(\frac{\tilde{\Sigma}_k^q + i\epsilon_{\mathbf{k}}}{2}\right)^2} - \frac{\tilde{\Sigma}_k^q + i\epsilon_{\mathbf{k}}}{2}, \tag{39}$$

where we choose the branch cut of the square root along the negative real axis. A similar expression, but at $\epsilon_{\mathbf{k}} = 0$ and at $\tilde{\Sigma}_k^q \approx \omega_m$ has been obtained in Ref. [29]. In Fig. 4(a), we plot the imaginary part of the total self-energy $\Sigma_k^{\text{th}} + \Sigma_k^q$ from Eqs. (36) and (39) as a function of $\epsilon_{\mathbf{k}}$ for different ω_m. The dependence is linear in $\epsilon_{\mathbf{k}}$ at the smallest ω_m, with the universal slope $-1/2$. This renormalizes the dispersion to $\epsilon_{\mathbf{k}}/2$. At larger ω_m, the renormalization of $\epsilon_{\mathbf{k}}$ becomes negligible. The crossover between the two regimes is at $\omega_m \sim B^{3/4}$ at the smallest T, and at $\omega_m \sim B$ at $T > (g^*)^3/E_F^2$. In Fig. 4(b) we plot Σ_k at $\epsilon_{\mathbf{k}} = 0$, where it is necessarily real. At the smallest $\omega_m \sim T$, Σ_k scales as $\omega_m^{2/3}$ at $B = 0$ and tends to a finite value $\Sigma_k \approx \sqrt{B}$ at a finite B.

We now substitute $\Sigma^{\text{th}}(\omega_m, \epsilon_{\mathbf{k}})$ from Eq. (39) into $\tilde{\Sigma}_k = \tilde{\Sigma}_k^q + \Sigma_k^{\text{th}}$ and then into Eq. (10) and explicitly integrate over $\epsilon_{\mathbf{k}}$. After some algebra (see Appendix B for details), we obtain that Σ^{th} *cancels out* from both terms in Eq. (10) which contain fermionic self-energy. Namely,

$$-T\sum_k \log\left[\epsilon_{\mathbf{k}}^2 + \tilde{\Sigma}_k^2\right] = -2\pi T N_F \sum_n |\omega_m + \Sigma^q(\omega_m)|,$$
$$2iT\sum_k \Sigma_k G_k = 2\pi T N_F \sum_n |\Sigma^q(\omega_m)|. \tag{40}$$

As a result Eq. (18) holds despite that the thermal self-energy depends on $\epsilon_{\mathbf{k}}$. For completeness, we verified explicitly that the momentum dependence of Σ^{th} does not generate a significant momentum dependence of Σ^q [which still contains the full self-energy in the Green's function in the r.h.s. of Eq. (6)].

A remark is in order here. In the analysis above we assumed that right above the nematic QCP, $T > T^*$, where $T^* \propto m_{\text{i-n}}^2$. When T^* by itself becomes a function of T due to T dependence of $m_{\text{i-n}}$, the condition $T > T^*$ may or may not hold. However, if the T dependence of $m_{\text{i-n}}$ is such that right above the QCP, $T < T^*$, the thermal self-energy depends only on frequency [Eq. (37)], and also cancels out in the free energy, as we demonstrated in Sec. II. We see therefore that the thermal self-energy cancels out in the free energy and the specific heat for any relation between T and T^*.

B. Strength of vertex corrections

The free energy in Eq. (10) is obtained within the self-consistent one-loop approximation, which neglects vertex corrections. Several authors argued [13,17,20,60–63] that at $T = 0$ lowest-order vertex corrections are generally of order one (or of order $1/N$ in large N theories), but higher-order corrections are $O(1)$ even at large N [20] and furthermore are logarithmically singular [60], except for special cases [64]. The logarithms, however, likely modify the quasiparticle residue but not the exponent $\gamma = 1/3$, and hence do not affect the $T^{2/3}$ behavior.

In this section, we estimate the strength of vertex corrections at a finite T. We recall that at a finite bosonic mass $m_{\text{i-n}}$, there is a range $T < T^*$, where $q_\parallel^{\text{typ}} \gg q_\perp^{\text{typ}}$ and the thermal self-energy $\Sigma^{\rm th} \sim g^* T/(m_{\text{i-n}} v_F)$ is obtained by factorizing the momentum integration between fermionic and bosonic propagators, and a range $T > T^*$, where the factorization does not hold. In this last regime, $\Sigma^{\rm th}$ generally depends on $\tilde{\Sigma}^q$ and $\epsilon_{\boldsymbol{k}}$ of an intermediate fermion. Within the self-consistent one-loop analysis, $\Sigma^{\rm th} \sim [g^* T \log(E_F/T)]^{1/2}$ At $m_{\text{i-n}} = 0$, $T^* = 0$, and the last regime holds for all T.

For $T < T^*$, a simple analysis shows that the leading vertex correction to fermion-boson coupling $\delta g^*/g^* \sim T/T^*$, i.e., it remains small in the same T range where one can factorize the momentum integration. For $T > T^*$, a similar analysis shows that $\delta g^*/g^* \sim g^* T \log(E_F/T)/(\tilde{\Sigma}_k)^2$. This vertex correction is at most of order one. It is then reasonable to expect that thermal vertex corrections do not modify $C(T) \propto T^{2/3}$ at a QCP, and, moreover, the prefactor differs from the one in Eq. (34) at most by a factor $O(1)$.

We emphasize that this holds even when vertex corrections shift the position of the maximum of the spectral function at k_F from $\omega = 0$ to a finite frequency. This may happen in a certain range of T above the QCP when self-energy and vertex corrections are treated on equal footings (see, e.g., Ref. [65] and references therein). In the latter case, the system displays a pseudogap behavior, yet the density of states at $\omega = 0$ remain finite. The $T^{2/3}$ of the specific heat then survives, albeit with a smaller prefactor.

C. Role of temperature dependence of $m_{\text{i-n}}$

We earlier included the T dependence of $m_{\text{i-n}}$ into the analysis of the thermal self-energy, which, we argued, does not contribute to the specific heat. However, the temperature-dependent $m^2_{\text{i-n}}$ also appears in the dressed bosonic propagator, and this temperature dependence does affect the free energy and the specific heat.

A regular temperature dependence of $m^2_{\text{i-n}}$ holds in powers of T^2. One can easily verify that it gives rise to a much weaker T dependence of $C(T)$ than $T^{2/3}$. A more subtle issue is the effect of the nonanalytic $T \log T$ dependence of $m^2_{\text{i-n}}$. The later comes from Fock-type one-loop thermal bosonic self-energy, assuming that there exists a T-independent coupling involving four bosonic fields. Such mode-mode coupling is a part of Hertz-Millis-Morya theory [58]. It has also been included into some recent studies of Ising-nematic QCP [34,56,59]. We computed the contribution to $C(T)$ from $m^2_{\text{i-n}} \propto T \log T$ and found that it gives rise to $T \log^2 T$ dependence of the specific heat. This T dependence is again subleading to $T^{2/3}$.

In 3D, the self-energy has the form typical for a marginal Fermi liquid: $\Sigma(\omega) \sim \omega \log \omega$, and the specific heat $C(T) \propto T \log T$.

IV. ANTIFERROMAGNETIC QCP IN 2D

The non-FL physics at a QCP toward spin order with momentum $\mathbf{Q} = (\pi, \pi)$ is described by the γ-model with $\gamma = 1/2$, as the self-energy in hot regions on the Fermi surface (the ones in which both $\epsilon_{\boldsymbol{k}}$ and $\epsilon_{\boldsymbol{k}+\boldsymbol{Q}}$ are small) scales as $\Sigma(\omega_m) \propto \omega_m^{1/2}$ [3,4].[2] The specific heat in the nonregularized γ-model scales as $\Lambda/\sqrt{T}$, and the one in the regularized γ-model scales as $\sqrt{T}$. Both are inconsistent with the specific heat of the underlying fermion-boson model $C_{\rm afm} \propto T \log T$, as we show below. The reason for the inconsistency is, however, rather banal—the non-FL behavior, described by the $\gamma = 1/2$ model, holds only in hot regions. Away from these regions the self-energy has a Fermi-liquid form at the smallest frequencies. Hot fermions contribute most to superconductivity, and the $\gamma = 1/2$ model of hot fermions adequately describes the interplay between non-FL and pairing. However, the free energy in the normal state is the combined contribution from fermions over the whole Fermi surface, and the one from hot fermions is proportional to the total width of the hot regions, which is small compared to the circumference of the Fermi surface boundary.

To obtain the specific heat, we compute the free energy using Eq. (10). We assume that Σ_k depends on frequency and on the position on the Fermi surface, but not on ϵ_k. In this situation, one can still explicitly integrate over the dispersion in the first two terms in Eq. (10). The result is that the self-energy cancels out, even if it depends on the momentum along the Fermi surface, and the free energy is given by Eq. (18). As before, we assume that D^0_q has Ornstein-Zernike form $D^0_q = -D_0/[(\mathbf{q}-\mathbf{Q})^2 + m^2_{\rm afm}]$ and incorporate the renormalizations from the static polarization bubble $\Pi(0)$ into $m_{\rm afm}$ and D_0. We evaluate the dynamical Landau damping term $\Pi(\Omega_m) - \Pi(0) = \alpha|\Omega_m|$ right at $\boldsymbol{q} = \boldsymbol{Q}$. The full propagator is

$$D_q = \frac{D_0}{(\mathbf{q}-\mathbf{Q})^2 + m^2_{\rm afm} + \alpha|\Omega_m|}. \tag{41}$$

Integrating over the component of $\mathbf{q} - \mathbf{Q}$ along the FS, we obtain

$$D_{\rm loc}(\Omega_m) = \frac{\bar{g}^{1/2}}{\left(\Omega_m^2 + M^2\right)^{1/4}}, \tag{42}$$

where $\bar{g}^{1/2} = g^2 D_0/(4\pi v_F \sqrt{\alpha})$ and $M \sim m^2_{\rm afm}$. This is Eq. (15) for $\gamma = 1/2$.

Substituting D_q from Eq. (41) into Eq. (18) and integrating over $\boldsymbol{q}$, we obtain

$$F_{\rm afm} = F_{\rm free} - \frac{3\alpha}{2} T^2 \sum_{n=1}^{M_B} n \log \frac{nT}{T_0}, \tag{43}$$

where the factor of 3 is due to summation over spin components and $T_0 \sim k_F^2/\alpha$ is a nonuniversal scale related to the upper cutoff of the integral over $\boldsymbol{q}$. Evaluating the frequency

[2]The actual value of γ is somewhat different from 1/2 as corrections to fermion-boson vertex are logarithmical, and series of these corrections change the exponent γ to $1/2 + \epsilon$, where ϵ is positive, but small numerically [4,75]. Besides, the dynamical exponent z also flows exponentially from $z = 2$ to a smaller value [26]. It has been argued [20] that in the absence of a superconducting instability, this flow eventually, at the lowest energies, brings the system into the basin of attraction of a stable fixed point with $z = 1$. Our analysis is valid at energies where the dynamical exponent is still $z \approx 2$.

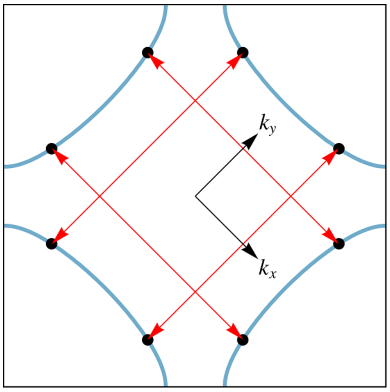

FIG. 5. Fermi surface (blue lines) and hot spots (black dots), connected by the ordering wave vector **Q** (red arrows). The coordinate frame (k_x, k_y) is used in the main text.

sum (see Appendix C 2 b for details) and using Eq. (32) to relate M_b and the energy cutoff Λ, we obtain

$$F_{\rm afm} = -\Lambda^2\left(N_F + \frac{3\alpha}{16\pi^2}\log\frac{\Lambda}{2\pi T_0\sqrt{e}}\right) + \frac{\pi^2}{3}T^2\left(-N_F + \frac{3\alpha}{8\pi^2}\log\frac{T}{T_0^*}\right), \tag{44}$$

where T_0^* differs from T_0 by a factor $O(1)$. Differentiating over T, we obtain

$$C_{\rm afm}(T) = S_{\rm afm}(T) = \frac{2\pi^2}{3}T\left(N_F + \frac{3}{8\pi^2}\alpha\log\frac{T_0^*}{Te^{3/2}}\right). \tag{45}$$

We see that at small T the interaction contribution to specific heat is larger than the one from free fermions, hence $C_{\rm afm}(T)$ scales as $T\log(T_0^*/T)$. This behavior has been extensively discussed in the context of non-FL behavior of cuprates and heavy fermion materials (see, e.g., Ref. [33] and references therein).

The prefactor α in Eqs. (44) and (56) can be expressed in terms of the effective electron-boson coupling g^* and Fermi velocities at hot spots $\boldsymbol{k}_{hs}$ and $\boldsymbol{k}_{hs}+\boldsymbol{Q}$. We define $\epsilon_{\boldsymbol{k}+\boldsymbol{k}_{hs}} = v_xk_x + v_yk_y$, $\epsilon_{\boldsymbol{k}+\boldsymbol{k}_{hs}+\boldsymbol{Q}} = v_xk_x - v_yk_y$ $(v_F^2 = v_x^2+v_y^2)$; see Fig. 5. In these notations [4],

$$\alpha = \frac{4g^*}{\pi v_F^2\beta}, \tag{46}$$

where $\beta = 2v_xv_y/v_F^2$. Substituting into Eq. (44), we obtain

$$C_{\rm afm}(T) = S_{\rm afm}(T) = \frac{2\pi^2}{3}N_FT\left(1 + \frac{3g^*}{2\pi^2E_F\beta}\log\frac{T_0^*}{Te^{3/2}}\right). \tag{47}$$

It is instructive to compare this result with the specific heat in a purely fermionic model with the self-energy averaged over the full Fermi surface. The self-energy at a Fermi point $k = k_F$, located at $\delta k_\parallel = \delta k$ from a hot spot, is [26,66]

$$\Sigma(\delta k, \omega_m) = \frac{3g^*}{4v_F}T\sum_{\Omega_m}\frac{\mathrm{sign}(\omega_m+\Omega_m)}{\sqrt{\alpha|\Omega_m| + (\beta\delta k)^2}}. \tag{48}$$

At $T = 0$,

$$\Sigma(\delta k, \omega_m) = \frac{3g^*}{2\pi v_F\alpha}\left(\sqrt{\alpha|\omega_m| + (\beta\delta k)^2} - \beta|\delta k|\right)\mathrm{sign}\omega_m. \tag{49}$$

At a hot spot, $\Sigma(0,\omega_m) \propto |\omega_m|^{1/2}$, as in the γ model with $\gamma = 1/2$. At the same time, the self-energy, averaged over δk, scales as $\log(T_0/|\omega_m|)$. Such a self-energy emerges in the γ-model with $\gamma = 0+$ [24,25,27,30,67,68] and hence proper comparison should be with this model. Indeed, substituting $\Sigma(\delta k, \omega_m)$ from Eq. (48) into Eq. (11), we obtain the free energy of the $\gamma = 0+$ model:

$$F_{0+} = F_{\rm free} - \frac{3g^*}{2\pi v_F^2\beta}T^2\sum_{n,n'}\mathrm{sign}(\omega_n\omega_{n'})\log\frac{T_0^{**}}{|\omega_n-\omega_{n'}|}, \tag{50}$$

where T_0^{**} is of the same order as T_0. The regularized free energy is

$$\bar{F}_{0+} = F_{\rm free} - \frac{3g^*}{2\pi v_F^2\beta}T^2\sum_{n,n'}[\mathrm{sign}(\omega_n\omega_{n'})-1]\log\frac{T_0^{**}}{|\omega_n-\omega_{n'}|}. \tag{51}$$

In Eqs. (50) and (51) the summation is over $-M_f < n, n' < M_f - 1$. Evaluating the sum and relating M_F to energy cutoff Λ via Eq. (21), we obtain

$$F_{0+} = -N_F\Lambda^2\left(1 + \frac{3g^*}{2\pi^2E_F\beta}\log 2\right) + N_F\frac{3g^*}{2\pi E_F\beta}\Lambda T\log\frac{T_0^{**}}{T} - \frac{\pi^2}{3}N_FT^2\left[1 + \frac{9g^*}{4\pi^2E_F\beta}\log\left(\frac{T_1}{T}\right)\right] \tag{52}$$

and

$$\bar{F}_{0+} = -N_F\Lambda^2\left(1 + \frac{3g^*}{2\pi^2E_F\beta}\log\frac{0.89\Lambda}{T_0^{**}}\right) - \frac{\pi^2}{3}N_FT^2\left[1 + \frac{3g^*}{2\pi^2E_F\beta}\log\left(\frac{T_1^*}{T}\right)\right], \tag{53}$$

where $T_1 \sim \Lambda$ and $T_1^* \sim \Lambda^2/T_0$. Differentiating with respect to temperature, we obtain

$$C_{0+}(T) = \frac{2\pi^2}{3}N_F\left\{\frac{9g^*}{4\pi^3E_F\beta}\Lambda + T\left[1 + \frac{9g^*}{4\pi^2E_F\beta}\log\left(\frac{T_1}{Te^{3/2}}\right)\right]\right\} \tag{54}$$

and

$$\bar{C}_{0+}(T) = S_{0+}(T) = \frac{2\pi^2}{3}N_FT\left(1 + \frac{3g^*}{2\pi^2E_F\beta}\log\frac{T_1^*}{Te^{3/2}}\right). \tag{55}$$

Comparing Eqs. (47) and (55) we see that the prefactor for the $T\log T$ term is the same. The outcome is that for an antiferromagnetic QCP the free energy of the purely electronic $\gamma = 0+$ model yields the same $C(T) \sim T\log T$ as the original fermion-boson model. This agrees with the analysis of Sec. III of the $\gamma = 1/3$ model, extended to arbitrary $0 < \gamma < 1$, where we found that the leading $T^{1-\gamma}$ terms in $\bar{C}_\gamma(T)$ and in the full $C(T)$ differ by a factor $1-\gamma$, which tends to one at $\gamma \to 0$. The specific heat in the nonregularized $\gamma = 0+$ model has a parasitic temperature-independent piece that scales with Λ. The prefactor for the universal $T \log T$ term in Eq. (54) is larger than the one in Eq. (55) by the factor 3/2—the same number as we found in Sec. III.

Away from the critical point, m_{afm} is finite, and at the smallest T the $\log(1/T)$ dependence in Eq. (44) is replaced by $\log(1/m^2_{\text{afm}})$. The total $C_{\text{afm}}(T)$ can then be cast in the form

$$C_{\text{afm}}(T) = \frac{2\pi^2}{3} N_F T \left(1 + \frac{3g^*}{\pi^2 E_F \beta} \log \frac{k_F}{m_{\text{afm}}}\right). \tag{56}$$

In this Fermi liquid regime, the self-energy, averaged along the Fermi surface, is $\Sigma_{\text{av}} = \lambda_{\text{av}}\omega$, where

$$\lambda_{\text{av}} = \frac{3g^*}{\pi^2 E_F \beta} \log \frac{k_F}{m_{\text{afm}}}. \tag{57}$$

Comparing Eqs. (56) and (57), we see that in a Fermi liquid regime at a finite m_{afm}, $C_{\text{afm}} = C_{\text{free}}(1 + \lambda_{\text{av}})$, which is the expected result.

The effects from thermal fluctuations and vertex corrections are similar to the Ising-nematic case. Namely, the thermal self-energy, obtained within self-consistent one-loop analysis does not contribute to the specific heat. Vertex corrections may give rise to pseudogap behavior above the QCP, but as long as the spectral function for $\mathbf{k}$ at the Fermi surface retains a finite value at $\omega = 0$, the $T \log T$ dependence of $C(T)$ survives, albeit with a smaller prefactor. Finally, we computed the contribution to $C(T)$ from mode-mode coupling and found that it also gives rise to $T \log T$ dependence (the larger $T \log^2 T$ contribution, which we found at the Ising-nematic QCP, cancels out at the antiferromagnetic QCP). As the consequence, $C(T) \propto T \log T$ survives, but the prefactor depends on the strength of mode-mode coupling.

In 3D, the self-energy of a hot fermion displays a marginal Fermi liquid behavior at a QCP, with $\Sigma(\omega) \sim \omega \log \omega$. For other $\mathbf{k}_F$ on the Fermi surface, the self-energy retains its Fermi liquid form. Averaging over $\mathbf{k}_F$, we find that the specific heat at a 3D antiferromagnetic QCP retains a Fermi liquid form $C(T) \sim T$.

V. QCP IN ELECTRON-PHONON SYSTEM

We now analyze the free energy for the case of electrons interacting with an Einstein boson. We use Eq. (18) as an input and compute the bosonic contribution to the specific heat. The propagator of an Einstein boson is $D_q = -D_0/(\Omega_m^2 + \omega_D^2 + \Pi_q)$, where ω_D is the bare Debye frequency and Π_q (which incorporates the overall factor D_0) comes from the interaction with electrons. We set ω_D to be finite, but much smaller than the Fermi energy $E_F = v_F k_F/2$. We define the dimensionless coupling λ via

$$\lambda = \frac{\bar{g}^2}{\omega_D^2}, \ \bar{g}^2 = g^2 N_F D_0, \tag{58}$$

where g is the same as in Eq. (5). We consider temperatures *smaller* than ω_D. At such T, the contribution to the specific heat from free bosons, $C_{\text{bos}} \propto e^{-\omega_D/T}$, is exponentially small.

For definiteness we consider the 2D case. The form of the 2D polarization operator of free fermions at small momentum and frequency is well known:

$$\Pi_q = 2\bar{g}^2\left(1 - \frac{\Omega_m}{\sqrt{\Omega_m^2 + (v_F q)^2}}\right). \tag{59}$$

We assume and then verify that typical $v_F q$ are of order E_F, while typical Ω_m for the specific heat are of order T. For such $v_F q$ and Ω_m, we can compute Π_q to linear order in Ω_m, but need a more accurate dependence on q. In 2D, the static part of Π_q remains equal to $2g^2$ for all momenta up to $2k_F$ and drops at larger momentum. The dynamical part changes between small q and $q \sim k_F$, and for arbitrary $q < 2k_F$ is

$$-2\bar{g}^2 \frac{|\Omega_m|}{v_F q} \frac{2k_F}{\sqrt{4k_F^2 - q^2}}. \tag{60}$$

Substituting Π_q at small Ω_m and arbitrary $q < 2k_F$ into D_q, we obtain

$$D_q^{-1} = \Omega_m^2 + \bar{\omega}_D^2 + 2\bar{g}^2 \frac{|\Omega_m|}{v_F q} \frac{2k_F}{\sqrt{4k_F^2 - q^2}}, \tag{61}$$

where $\bar{\omega}_D = \omega_D(1 - 2\lambda)^{1/2}$ is the dressed Debye frequency. The dressed $\bar{\omega}_D$ vanishes at $\lambda = 1/2$ for all momenta $q < 2k_F$. At larger q, the static Π_q decreases and $\bar{\omega}_D$ remains finite even at $\lambda = 1/2$.

Strictly speaking, the polarization operator has to be computed using full fermionic propagators, which include the self-energy. This does affect the static Π_q, which is generally different from $2g^2$ and has contributions from fermions with energies of order E_F, of the order of the upper cutoff Λ in the γ model [69]. To simplify the discussion, below we keep the free-fermion result with the understanding that the actual renormalization of ω_D likely differs somewhat from $(1 - 2\lambda)^{1/2}$. The corrections to the Landau damping term $|\Omega_m|/v_F q$ is of order of λ_E and hence are small. We assume without proof that this holds even when we extend the Landau damping formula to $q \sim k_F$.

We show below that within the regime of validity of the Eliashberg theory, $\lambda_E \ll 1$, the last term in Eq. (61) is small compared to the first two. The corresponding γ model then has $\gamma = 2$.

The vanishing of the dressed Debye frequency at some finite λ ($\lambda = 1/2$ if we use free-fermion expression for static Π_q) has been noticed before (see, e.g., Refs. [12,41,70] and references therein), both in 2D and 3D systems. However, in 3D, $\bar{\omega}_D$ is not flat for $q < 2k_F$, and the dressed $\bar{\omega}_D$ vanishes at a critical λ only at $q = 0$ and scales as q^2 at small q. In this situation the full bosonic propagator has the same form as in the 3D Ising-nematic model, and the corresponding γ model has $\gamma = 0+$, with the effective interaction

$$D_{\text{loc}}(\Omega_m) = \log \frac{\bar{g}}{|\Omega_m|}. \tag{62}$$

In 2D, corrections to free-fermion form of Π_q also introduce quadratic momentum dependence of $\bar{\omega}_D$ around $q = 0$, even for an isotropic fermionic dispersion [71], such that very near QCP critical theory becomes the same as in a 2D Ising-nematic case. Alternatively, a nonparabolic fermionic dispersion can also introduce a quadratic term in the bosonic dispersion. However, the momentum dependence may be weak, resulting in a wide range around a QCP, where $\bar{\omega}_D$ can be approximated by momentum-independent constant, $\omega_D(1-2\lambda)^{1/2}$. For a system on a square lattice, quantum Monte Carlo data show that the minimum of $\bar{\omega}_D$ is at $M = (\pi,\pi)$ [72]. The dispersion is flat around the minimum, and the overall variation of $\bar{\omega}_D$ with momentum is quite small. At the minimum, $\bar{\omega}_D$ displays $(1-2\lambda)^{1/2}$ dependence up to $\lambda \sim 0.4$ [12].

In our analysis of the free energy we focus on the regime where the momentum dependence of $\bar{\omega}_D$ can be neglected. In this regime $F = F_{\text{free}} + (T/2)\sum_q \log(-D_q^{-1})$, where $F_{\text{free}} = -\pi^2T^2N_F/3$ is the free energy of a free Fermi gas. We assume and then verify that the largest contribution to the specific heat comes from the $\boldsymbol{q}$-independent term in D_q and approximate $\log(-D_q^{-1})$ by expanding to leading order in the Landau damping term (which we shall later show is a small correction for an $\gamma > 1$),

$$\log\left(-D_q^{-1}\right) = \log\left(\Omega_m^2+\bar{\omega}_D^2\right) + 2\frac{\bar{g}^2}{v_F q}\frac{|\Omega_m|}{\Omega_m^2+\bar{\omega}_D^2}\frac{2k_F}{\sqrt{4k_F^2-q^2}}. \tag{63}$$

Substituting into the free energy and integrating over $|\mathbf{q}| < 2k_F$, we obtain

$$\frac{T}{2}\sum_q \log\left(-D_q^{-1}\right) = \frac{k_F^2}{\pi}T\sum_{n=1}^{M_b}\log\left(4\pi^2T^2n^2+\bar{\omega}_D^2\right) + \frac{\bar{g}^2k_F}{2\pi v_F}\sum_{n=1}^{M_b}\frac{n}{n^2+[\bar{\omega}_D/(2\pi T)]^2}. \tag{64}$$

The first term is the free energy of a free Einstein boson with the renormalized Debye frequency $\bar{\omega}_D$, the second one is the contribution from fermion-boson interaction. Evaluating the frequency sums (see the Appendix C 2 c for details) and using the relation between M_b and the upper energy cutoff Λ, Eq. (32), we obtain

$$F = N_F\left(-\Lambda^2 + \frac{4E_F\Lambda}{\pi}\log\frac{\Lambda}{e} + \bar{g}^2\log\frac{\Lambda}{\bar{\omega}_D}\right) + N_F\left[-\frac{\pi^2T^2}{3} + 4TE_F\log\left(1-e^{-\frac{\bar{\omega}_D}{T}}\right) + \bar{g}^2 f\left(\frac{\bar{\omega}_D}{2\pi T}\right)\right], \tag{65}$$

where

$$f(x) = \log x - \tfrac{1}{2}[\psi(1+ix)+\psi(1-ix)], \tag{66}$$

and $\psi(y)$ is digamma function. We see that the Λ-dependent terms in Eq. (65) are independent of T, and hence do not contribute to the entropy and the specific heat. Differentiating twice with respect to temperature, we obtain the total specific heat for the isotropic electron-phonon system

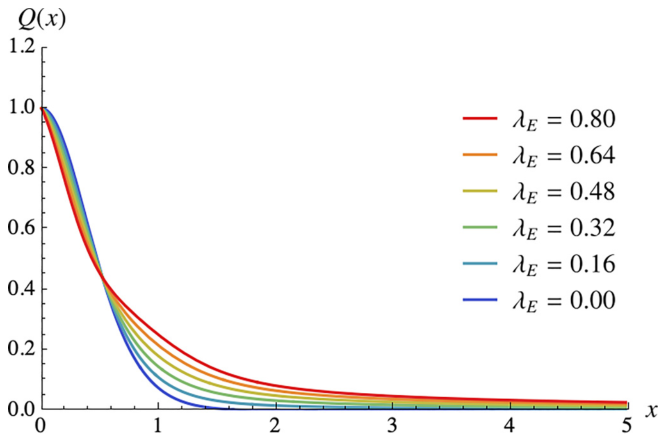

FIG. 6. Function $Q(x)$, given by Eq. (68), for different $\lambda_E < 1$.

$$C_{\text{ep}}(T) = \frac{2\pi^2}{3}N_F\left[T + \frac{6E_F}{\pi^2}Q\left(\frac{\bar{\omega}_D}{2\pi T}\right)\right], \tag{67}$$

where

$$Q(x) = \left(\frac{\pi x}{\sinh \pi x}\right)^2 - \frac{\pi}{2}\lambda_E x^2\left(x\frac{d^2f}{dx^2} + 2\frac{df}{dx}\right), \tag{68}$$

and $\lambda_E = \bar{g}^2/(\bar{\omega}_D E_F)$ is the Eliashberg parameter. The Elishberg theory, which neglects vertex corrections, is valid when λ_E is small. In Fig. 6, we plot $Q(x)$ for different λ_E. We see that this function is positive for all x. Accordingly, $C_{\text{ep}}(T)$ given by Eq. (66) is also positive for all temperatures. We plot $C(T)$ in Fig. 7.

The limiting forms of $C_{\text{ep}}(T)$ are

$$C_{\text{ep}}(T) = \frac{2\pi^2}{3}N_F T\left(1 + \frac{\lambda}{1-2\lambda}\right) \tag{69}$$

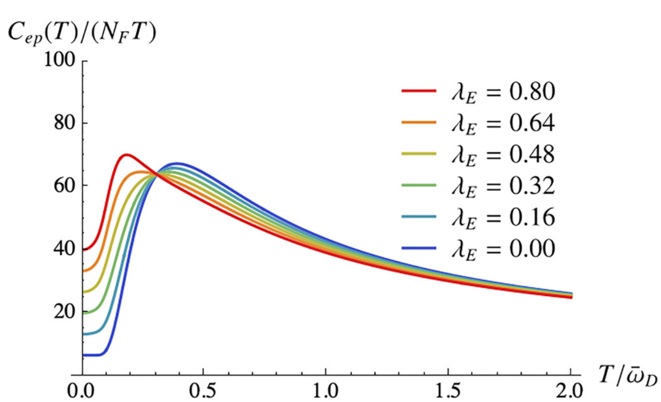

FIG. 7. The ratio $C_{\text{ep}}(T)/T$, where $C_{\text{ep}}(T)$ is the specific heat of the electron-phonon system, given by Eq. (67). We plot $C(T)/T$ a function $T/\bar{\omega}_D$, where $\bar{\omega}_D$ is the dressed Debye frequency, for different values of the Eliashberg parameter λ_E. We set $E_F = 10\bar{g}$, in which case $\lambda_E = 0.1(\bar{g}/\bar{\omega}_D)^2$. The specific heat is positive at all T. At $T \ll \bar{\omega}_D$, $C_{\text{ep}}(T)/T$ saturates at $2\pi^2/3N_F[1+\lambda/(1-2\lambda)]$ at $T \gg \bar{\omega}_D$, $C_{\text{ep}}(T)/T$ asymptotically approaches its value for free bosons.

at $2\pi T \ll \bar{\omega}_D$, and

$$C_{\rm ep}(T) = \frac{2\pi^2}{3}N_F\left[T + \frac{6E_F}{\pi^2}\left(1-\lambda_E\frac{\bar{\omega}_D}{4T}\right)\right] = \frac{2\pi^2}{3}N_F\left(T + \frac{6E_F}{\pi^2} - \frac{3\bar{g}^2}{2\pi^2 T}\right) \quad (70)$$

at $2\pi T \gg \bar{\omega}_D$, which includes the case $\bar{\omega}_D \to 0$ at finite T. In the two limits, the entropy $S_{\rm ep}(T) = C_{\rm ep}(T)$ at $2\pi T \ll \bar{\omega}_D$, and

$$S_{\rm ep}(T) = \frac{2\pi^2}{3}N_F\left(T + \frac{6E_F}{\pi^2}\log\frac{T}{\bar{\omega}_D} + \frac{3\bar{g}^2}{2\pi^2 T}\right) \quad (71)$$

at $2\pi T \gg \bar{\omega}_D$. Note that in this last limit the entropy is always positive. It diverges logarithmically at $\bar{\omega}_D \to 0$ at a finite T.

We now take a more careful look at the expression for the specific heat at $2\pi T \gg \bar{\omega}_D$. The first term in the second line in Eq. (70) is the contribution from free fermions, the second is the contribution from free bosons, but with an effective Debye frequency, renormalized by the interaction with fermions, and the third term is the direct contribution from the electron-phonon interaction. This last term is negative and is the same as the interaction contribution to the specific heat in the regularized γ model [Eq. (28)]. Without the middle term, the specific heat would become negative below a certain temperature, $T = [3/(2\pi^2)]^{1/2}\bar{g} \simeq 0.39\bar{g}$, which exceeds the onset temperature for superconductivity $T_c \simeq 0.18\bar{g}$ [35,73,74]. Because of the middle term, however, the full $C(T)$ remains positive, The key here is the condition $\lambda_E = \bar{g}^2/(\bar{\omega}_D E_F) < 1$, which requires one to treat the case of vanishing dressed Debye frequency as a double limit, in which E_F tends to infinity simultaneously with $\bar{\omega}_D \to 0$ [37,38]. We plot the full $C_{\rm ep}(T)$ from Eq. (67) in Fig. 7. We see that it is indeed positive for $\lambda_E < 1$.

The authors of Refs. [40,41] argued that the negative prefactor for the $1/T$ term in Eq. (28) indicates that the normal state becomes unstable below a certain T despite that the total $C_{\rm ep}(T)$ is positive. Their argument is that the T-independent term in Eq. (70), which renders the total $C_{\rm ep}(T)$ positive, is the contribution from free bosons and as such does not affect the electrons. Our counterargument is that both positive and negative parts of $C_{\rm el}(T)$ come from the term in the free energy $(T/2)\sum_q \log[-D_q^{-1}]$, once one expands it in the dynamical part of Π_q: the positive contribution is the zeroth-order term and the negative $1/T$ contribution comes from the first order in the expansion. In our view, this shows that both terms should be treated on equal footings. Besides, despite the fact that the leading T-independent part of $C_{\rm el}(T)$ has the same form as the specific heat of a free massless boson, this term does depend on fermion-boson interaction as the latter renormalizes the bare ω_D into $\bar{\omega}_D = \omega_D\sqrt{1-2\lambda}$. For $\lambda \approx 1/2$, $\omega_D = \bar{g}/\sqrt{\lambda} \approx \sqrt{2}\bar{g}$ is comparable to $\bar{g}$, and without interaction-driven renormalization of ω_D into $\bar{\omega}_D$ the specific heat of free bosons would be exponentially small at $T \leqslant \bar{g}$. In this respect, the fermion-boson coupling gives rise to two effects: it generates a negative T-dependent contribution to $C_{\rm ep}$, and simultaneously gives rise to a much larger, positive T-independent contribution.

For completeness, we also computed the specific heat within our model for larger λ_E, using the full formula for $\log D_q^{-1}$ rather than expanding in the Landau damping in Eq. (63). We found that the specific heat is positive for all λ_E. We plot $C_{\rm ep}/T$ in Fig. 8. This result is of limited validity, however, as in the free energy we did not include higher-order terms in the skeleton expansion in $F_{\rm int}$. These terms are of higher order in λ_E, when λ_E is small, but are not small when $\lambda_E > 1$. Still, we emphasize that within the model that we used here, $C_{\rm ep}(T)$ is positive for all T.

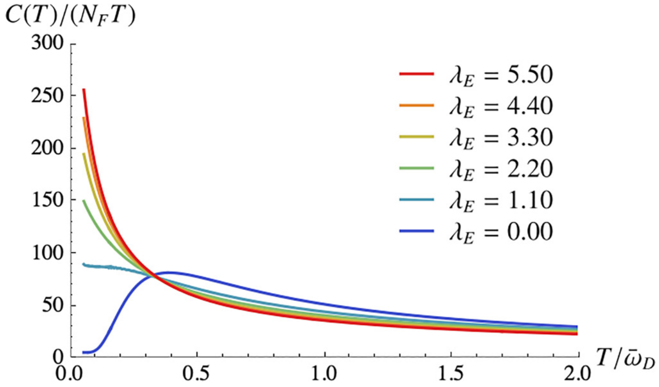

FIG. 8. Normalized specific heat of the electron-phonon system, $C_{\rm ep}(T)/T$, obtained by using the full expression for the free energy $F = F_{\rm free} + (T/2)\sum_q \log(-D_q^{-1})$, without expanding $\log(-D_q^{-1})$ in the Landau damping. We used the same parameters as in Fig. 7. The specific heat remains positive for all values of λ_E.

In 3D the polarization bubble depends on momenta as q^2 at small q, and the full bosonic propagator for electron-phonon problem has the same form as in the 3D Ising-nematic model (and the γ-model at $\gamma = 0+$), see the discussion around Eq. (62). Accordingly, the specific heat displays marginal Fermi liquid behavior $C(T) \sim T\log T$.

A. Physical origin of the regularization of F_γ

We now argue that the interaction-driven renormalization of ω_D is related to the issue of the regularization of F_γ in the γ model. To relate the two, we recall that $iT\sum_k \Sigma_k G_k$, which is the interaction part of F_γ, can be re-expressed as $(T/2)\sum_q \Pi_q D_q$ [see Eq. (8)], where $q = (\mathbf{q}, \Omega_m)$ and $\Pi_q = 2g^2 T\sum_k G_k G_{k+q}$. In the analysis above, we computed this last term neglecting in D_q the dynamical part of Π_q, which also depends on momentum $\mathbf{q}$. Without this term, D_q depends only on frequency, and the momentum integration involves only Π_q. The double integral over $\mathbf{q}$ and $\mathbf{k}$ can be transformed into the integration over the two fermionic momenta $\mathbf{k}$ and $\mathbf{k}+\mathbf{q}$ and then into the integration over the two dispersions ϵ_k and ϵ_{k+q}. Each integral is proportional to signω_m, where ω_m is the Matsubara frequency in the corresponding Green's function, hence the momentum integration gives rise to the factor sign$(\omega_m\omega_{m'})$, where $\omega_m - \omega_{m'} = \Omega_m$. This is the same factor as in the second term in Eq. (20) for the free energy F_γ of the nonregularized γ model. The same holds for the interaction term in the free energy in the γ model: sign$(\omega_m\omega_{m'})$ in the interaction term in Eq. (20) has been obtained by integrating independently over two fermionic dispersions: one of G_{k-q} in Eq. (6) and the other of G_k in $iT\sum_k \Sigma_k G_k$. Using now

$\text{sign}(\omega_m\omega_{m'}) = 1 + [\text{sign}(\omega_m\omega_{m'}) - 1]$, we immediately see that the first and second terms correspond to contributions from the static and dynamical parts of Π_q, respectively.

Hence, the static part of Π_q accounts for the renormalization of the bare ω_D into $\bar{\omega}_D$, which vanishes at the QCP. In the underlying fermion-boson model, Π_q is the full polarization operator, with static and dynamics parts, and the renormalization $\omega_D \to \bar{\omega}_D$ must be taken into consideration. This implies that $(T/2)\sum_q \Pi_q D_q$ and $iT\sum_k \Sigma_k G_k$ have to be computed without adding counter terms, and both depend on the upper cutoff. Like we demonstrated, the two terms cancel out in the full free energy F. The latter is expressed in terms of D_q^{-1}, which contains the dressed $\bar{\omega}_D$ and the dynamical part of Π_q.

Then even when the renormalization of the bosonic mass does depend on the cutoff (e.g., in the case of a lattice dispersion), the free energy is expressed via the fully dressed mass, which vanishes at a QCP.

The γ model is constructed differently. In this model, the renormalization of ω_D into $\bar{\omega}_D$ is already absorbed into $D_{\text{loc}}(q)$, which, by construction, depends on the dressed $\bar{\omega}_D$. Hence, the terms which renormalize ω_D must be excluded to avoid double counting. The way to do this is to eliminate the contribution from the static part of Π_q by replacing $\text{sign}(\omega_m\omega_{m'})$ by $\text{sign}(\omega_m\omega_{m'}) - 1$. This is precisely the counter term, which the authors of Refs. [40–42] suggested to add to regularize the free energy of the γ model.

The same reasoning holds for other values of γ. In each γ model, one has to subtract the renormalization of the bosonic mass to avoid double counting. This is achieved by the same substitution $\text{sign}(\omega_m\omega_{m'})$ by $\text{sign}(\omega_m\omega_{m'}) - 1$ in Eq. (20).

VI. EXTENSION TO $\gamma < 2$

It is instructive to verify how the T independent and the $1/T$ term in Eq. (70) evolve if we add a momentum-dependent term to the bosonic propagator D_q in Eq. (61) and gradually change the exponent γ in the corresponding γ model to $\gamma < 2$. A way to do this phenomenologically is to consider a fermion-boson model with the bosonic propagator

$$D_q^{-1} = \Omega_m^2 + (cq)^{2a} + \bar{\omega}_D^2 + 2\bar{g}^2\frac{|\Omega_m|}{v_F q}, \tag{72}$$

with $a > 1$. We assume that the q^{2a} term comes from fermions with energies of order E_F, and set the prefactor c to be of order $E_F^{1/a}/k_F$. As before, we consider the double limit in which $\bar{\omega}_D$ tends to zero and simultaneously E_F tends to infinity.

We verified that the leading contribution to the fermionic self-energy $\Sigma(\omega_m)$ comes from the first two terms in Eq. (72), while the Landau damping term accounts for a negative correction. Specifically,

$$\Sigma(\omega_m) \propto |\omega_m|^{1/a-1}\left[1 - \left(\frac{T_a}{|\omega_m|}\right)^{\frac{a+1}{a}}\right], \tag{73}$$

where

$$T_a \sim \bar{g}\left(\frac{\bar{g}}{E_F}\right)^{\frac{a-1}{a+1}}. \tag{74}$$

For $E_F \to \infty$, T_a tends to zero, hence $T_a/|\omega_m|$ is vanishingly small for all ω_m. Comparing Eq. (73) with $\Sigma(\omega_m) \propto |\omega_m|^{1-\gamma}$ in the γ model, we find $\gamma = 2 - 1/a$. This exponent ranges between 1 and 2, when a ranges between 1 and infinity. At $a = 1 + 0$, a more accurate analysis shows that $\Sigma(\omega_m) \propto \log|\omega_m|$.

The free energy and the specific heat can be obtained in the same way as above. For brevity, we skip the details of the calculations and just list the results. We also neglect the free-fermion part of the specific heat and label the specific heat due to fermion-boson interaction as $C_{\text{int}}(T)$. Up to a positive overall factor,

$$C_{\text{int}}(T) \propto T^{\frac{2}{a}}\left[1 - \left(\frac{T_a}{T}\right)^{\frac{a+1}{a}} + \cdots\right], \tag{75}$$

where dots stand for higher-order terms in the expansion in T_a/T. The positive term in Eq. (75) comes from the Ω_m^2 and $(cq)^{2a}$ terms in the bosonic propagator, and the negative term comes from the Landau damping term in Eq. (72). This negative term is vanishingly small as T_a tends to zero when $a > 1$. The exponent $1/a$ equals to $2 - \gamma$, hence $C_{\text{int}}(T) \propto T^{2(2-\gamma)}$. For $\gamma = 2$, $C_{\text{int}}(T)$ becomes temperature independent. This is consistent with the result that we obtained in the previous section.

A. Extension to $1/2 < a < 1$

For completeness, we also present the results for smaller values of the exponent a: $1/2 < a < 1$. The condition $a > 1/2$ is required for ultraviolet convergence.

Evaluating the fermionic self-energy, we now obtain

$$\Sigma(\omega_m) \propto |\omega_m|^{\frac{2}{2a+1}}\left[1 - \left(\frac{|\omega_m|}{T_a}\right)^{\frac{a+1}{a}}\right], \tag{76}$$

where T_a is the same as in Eq. (74). The dominant contribution to the self-energy now comes from the Landau damping term and from the $(cq)^{2a}$ term in D_q in Eq. (72), while the Ω_m^2 term accounts for a negative correction. Because T_a now tends to infinity at $E_F \to 0$, the second term in Eq. (56) is vanishingly small for all ω_m. Associating the exponent $2/(2a+1)$ with $1-\gamma$, we find that for $a < 1$, $\gamma = (2a-1)/(2a+1)$.

For the specific heat we find

$$C_{\text{int}}(T) \propto T^{\frac{2}{2a+1}}\left[1 - \left(\frac{T}{T_a}\right)^{\frac{a+1}{a}} + \cdots\right]. \tag{77}$$

The positive contribution to $C(T)$ now comes from the Landau damping term and the $(cq)^{2a}$ term in Eq. (72), while the negative contribution comes from the Ω_m^2 term. The dots stand for terms with higher powers of T/T_a. Because for $a < 1$, T_a tends to infinity at $E_F \to \infty$, the negative term is vanishingly small at any T. As a result $C_{\text{int}}(T)$ is again positive. Using the relation $\gamma = (2a-1)/(2a+1)$, valid for $a < 1$, we find that $C_{\text{int}}(T) \propto T^{1-\gamma}$. This agrees with the results in Sec. (III). At $a \to 1/2$, a more accurate analysis yields $C_{\text{int}}(T) \propto T\log T$, as in Sec. (IV).

There is a discontinuity in γ at $a = 1$, i.e., the model with $a = 1 + 0$ corresponds to $\gamma = 1$, and the one with $a = 1 - 0$ corresponds to $\gamma = 1/3$. This is the consequence of discontinuity of T_a at $a = 1$ and $E_F \to \infty$: T_a tends to zero at $a > 1$, is of order $\bar{g}$ at $a = 1$, and tends to infinity at $a < 1$. Right at $a = 1$, the frequency dependence of the self-energy and the temperature dependence of the specific heat undergo a crossover from $\Sigma(\omega_m) \propto |\omega_m|^{2/3}$ and $C_{\rm int}(T) \sim T^{2/3}$ at $\omega_m, T \ll \bar{g}$ to $\Sigma(\omega_m) \propto \log|\omega_m|$ and $C_{\rm int}(T) \sim T^2$ at $\omega_m, T \gg \bar{g}$ (modulo logarithms). In both cases the specific heat is positive. The low-temperature behavior of the model with $a = 1$ is the same as in the $\gamma = 1/3$ model.

VII. CONCLUSIONS

In this paper, we analyzed the free energy and specific heat for a system of fermions interacting with nearly gapless bosons near a QCP in a metal. The effective low-energy model for quantum-critical fermions is the one in which bosons are integrated out, and the fermions are interacting via an effective, purely dynamical interaction $V(\Omega_m) \propto 1/|\Omega_m|^\gamma$. This γ model is adequate for the description of non-FL behavior and pairing near a QCP, and the competition between tendencies toward non-FL and pairing. This physics is fully determined by low-energy fermions and is independent on the upper energy cutoff in the theory, Λ. The condensation energy, associated with pairing, is also independent of Λ. At the same time, the free energy the γ model in the normal state does depend on Λ. Furthermore, this extends to temperature-dependent terms in the free energy. As a result, the specific heat in the γ model also depends on the cutoff. In recent papers [41,42], the authors argued that the dependence of $C_\gamma(T)$ on Λ is a spurious one and has to be eliminated by proper regularization. They added a term to the free energy, which cancels out cutoff dependence of the free energy. However, the regularized $C_\gamma(T)$ turns out to be negative for large enough γ [38,41,42]

Here, we analyzed the specific heat near the QCP by returning back to the underlying fermion-boson model and collecting contributions to the free energy from fermions, bosons, and their interaction. This allowed us to obtain the full expression for the specific heat and compare it with the specific heat in the γ model.

Our key result is that the specific heat in the full fermion-boson model is independent on the cutoff and is positive all the way up to a QCP.

We considered three cases, all in 2D: Ising-nematic QCP, antiferromagnetic QCP, and QCP for electrons interacting with Einstein phononons. For the first case, the exponent in the purely electronic model is $\gamma = 1/3$. For the second it is $\gamma = 1/2$ for fermions near the hot spots, but is reduced to $\gamma = 0+$ in the effective model with the interaction averaged over the Fermi surface. For electron-phonon case, the effective fermion-only model has $\gamma = 2$.

For the two cases with $\gamma < 1$ the specific heat in the regularized γ-model is positive. We found that the regularization and the effect of keeping the bosonic piece in the free energy is largely the same thing. Specifically, the regularized specific heat C_γ has correct temperature dependence ($T^{2/3}$ for the Isng-nematic case, and $T\log T$ for the AFM case), and the prefactor differs from the correct one only by a numerical factor, which, moreover, is equal to one in the AFM case.

In the electron-phonon case ($\gamma = 2$) the modified electronic specific heat reproduces the temperature dependence of the actual $C(T)$. However, $C(T)$ has an additional temperature-independent piece, which also comes from the electron-phonon interaction. We found that the full $C(T)$ is positive as long as the dimensionless Eliashberg parameter λ_E, which measures the strength of vertex corrections, is small. We verified that the same holds for other models, for which the regularized C_γ is negative.

We believe that a positive total $C(T)$ implies that the normal state of a critical fermion-boson model remains stable at all T, as long as one neglects the pairing instability.

The authors of Ref. [41] also found that the total specific heat of the electron-phonon model is positive. They, however, argued that a negative C_γ already implies that the system is unstable because electronic and bosonic contributions are independent on each other. Our argument for stability is that both contribution come from the same $T\sum_q \log D_q^{-1}$ term in the free energy. A positive part of $C(T)$ comes from taking D_q^{-1} without the Landau damping, and the negative part comes from the Landau damping.

ACKNOWLEDGMENTS

We thank Ar. Abanov, B. Altshuler, A. Klein, A. Levchenko, D. Maslov, J. Schmalian, G. Torroba, Y. Wang, Y. Wu, and E. Yuzbashyan for fruitful discussions. This project was supported by the U.S.-Israel Binational Science Foundation (BSF). The work by A.V.C. was supported by U.S. Department of Energy, Office of Science, Basic Energy Sciences, under Award No. DE-SC0014402. E.B. was supported by the European Research Council (ERC) under grant HQ-MAT (Grant Agreement No. 817799).

APPENDIX A: DETAILS ABOUT ISING-NEMATIC CASE

1. Self-energy of an electron at a finite *T*

The one-loop self-energy of an electron is given by

$$i\Sigma_k = -g^* T \sum_{\Omega_m} \int \frac{d^2\boldsymbol{q}}{(2\pi)^2} \frac{1}{i\tilde{\Sigma}_{k+q} - \epsilon_{\boldsymbol{k}+\boldsymbol{q}}} \frac{D_0}{q^2 + m^2 + \alpha\frac{|\Omega_m|}{|\boldsymbol{q}|}}, \tag{A1}$$

where $\Sigma_k = \Sigma(\mathbf{k}, \omega_m)$ and the notations are the same as in the main text: $\tilde{\Sigma}_k \equiv \omega_m + \Sigma_k$ and $\alpha = g^* k_F/(\pi v_F^2)$, where g^* is the effective fermion-boson coupling.

At $T = 0$, the sum is replaced by $T\sum_{\Omega_n} = (1/2\pi)\int d\Omega_n$. The leading term in Σ_k is obtained by factorizing the momentum integration along and transverse to the Fermi surface (see Fig. 3 of the main text). This leading term depends only on frequency, i.e., the self-energy is local. At a QCP,

$$\Sigma_k = \tfrac{3}{2}\bar{g}^{1/3}|\omega_m|^{2/3}\mathrm{sgn}(\omega_m), \tag{A2}$$

where $\bar{g}$—the coupling constant of the corresponding fermionic $\gamma = 1/3$ model—is

$$\bar{g} = \frac{1}{3^{9/2}}\left(\frac{v_F}{k_F}\right)^3 \alpha^2 = \frac{1}{3^{9/2}\pi^2}\frac{(g^*)^2}{E_F}. \tag{A3}$$

The factorization of momentum integration is valid as long as typical fermionic momenta $q_f^{\rm typ} \sim \max(\tilde{\Sigma}(\omega_m), \epsilon_{\boldsymbol{k}})/v_F$ (same as typical momenta transverse to the Fermi surface $q_\perp^{\rm typ}$) is much smaller than typical bosonic momentum $q_b^{\rm typ} \sim (\alpha|\Omega_m|)^{1/3}$ (same as typical momenta along the Fermi surface

$q_\parallel^{\rm typ}$). The comparison of the two scales shows that the factorization is valid in the whole range where $\Sigma_k > \omega_m$ and at larger frequencies holds up to $\omega_{\max} \sim (g^* E_F)^{1/2} \sim \bar{g}^{1/4} E_F^{3/4}$.

At a finite temperature, there are two types of bosonic fluctuations: the thermal one with $\Omega_m = 0$ and the quantum one with $\Omega_m \neq 0$. This splits the self-energy into two parts [4,23,29,31,34]:

$$\Sigma_k(k) = \Sigma_k^{\rm th} + \Sigma_k^q, \tag{A4}$$

where, we remind, $\Sigma_k = \Sigma(\mathbf{k}, \omega_m)$. We have

$$i\Sigma^{\rm th}(\mathbf{k}, \omega_m) = -g^* T \int \frac{d^2\boldsymbol{q}}{(2\pi)^2} \frac{1}{i\tilde{\Sigma}(\boldsymbol{k}+\boldsymbol{q}, \omega_m) - \epsilon_{\boldsymbol{k}+\boldsymbol{q}}} \times \frac{1}{|\boldsymbol{q}|^2 + m^2}, \tag{A5}$$

and

$$i\Sigma^q(\mathbf{k}, \omega_m) = -g^* T \sum_{\Omega_n \neq 0} \times \int \frac{d^2\boldsymbol{q}}{(2\pi)^2} \frac{1}{i\tilde{\Sigma}(\boldsymbol{k}+\boldsymbol{q}, \omega_m + \Omega_m) - \epsilon_{\boldsymbol{k}+\boldsymbol{q}}} \times \frac{1}{|\boldsymbol{q}|^2 + m^2 + \alpha \frac{|\Omega_n|}{|\boldsymbol{q}|}}. \tag{A6}$$

Below we consider the two components of the self-energy separately. We assume for simplicity that the bosonic mass m acquires some weak temperature dependence via mode-mode coupling and cut $\log m$ singularity in the formulas below by $\log T$ (for the analysis of Σ_k for T-independent mass, see Ref. [29]. In this approximation, the quantum self-energy Σ^q can still be computed by factorizing the momentum integration and remain local [29,56]. The result is

$$\Sigma^q(\omega_m) = \pi T \sum_{\Omega_n \neq 0} \left(\frac{\bar{g}}{|\Omega_n|}\right)^{1/3} \mathrm{sgn}(\omega_m + \Omega_n) = \bar{g}^{1/3} (2\pi T)^{2/3} H_{1/3}(m), \tag{A7}$$

where $H_\gamma(m) = \sum_{n=1}^m 1/n^\gamma$ is the Harmonic number. At frequencies $\omega_m \gg T$, one can use the expansion of a Harmonic number at large m: $H_{1/3}(m) \simeq 3/2(m+1/2)^{2/3} + \zeta(1/3) + \cdots$ and obtain

$$\Sigma^q(\omega_m) \simeq \tfrac{3}{2} \bar{g}^{1/3} \mathrm{sgn}(\omega_m) \times \left[|\omega_m|^{2/3} + \tfrac{2}{3}\zeta(1/3)(2\pi T)^{2/3} + \cdots\right]. \tag{A8}$$

This formula is valid up to the same $\omega_{\max}$ as at $T = 0$.

For thermal self-energy, momentum integration can be factorized only in a particular parameter range, which we identify below. Outside this range, the leading contribution to $\Sigma_k^{\rm th}$ in Eq. (A5) is obtained by integrating over both momentum components in the bosonic propagator.

Below we consider separately parameter ranges where $\Sigma_k^{\rm th}$ is local and where it is not.

2. Local self-energy: $\Sigma_k \equiv \Sigma(\omega_m)$

In this section, we consider the situation when the momentum integration in Eq. (A5) can be factorized. The factorization implies that for the same frequency, typical fermionic momentum (the one transverse to the Fermi surface) is much smaller than typical bosonic momentum connecting points on the Fermi surface. Typical fermionic momentum is $q_f^{\rm typ} \sim \max(\tilde{\Sigma}(\omega_m), \epsilon_{\boldsymbol{k}})/v_F$, while typical bosonic momentum is $q_b^{\rm typ} \sim m$. Factorization is justified when $q_f^{\rm typ} \ll q_b^{\rm typ}$. Under this condition

$$i\Sigma^{\rm th}(\omega_m) = -\frac{g^* T}{4\pi^2} \int_{-\Lambda_q}^{\Lambda_q} \frac{dq_\perp}{i\tilde{\Sigma}(\omega_n) - \epsilon_{\boldsymbol{k}} - v_F q_\perp} \int_{-\Lambda_q}^{\Lambda_q} \frac{dq_\parallel}{q_\parallel^2 + m^2}, \tag{A9}$$

where $\Lambda_q \sim k_F$ is the upper cutoff of momentum integration. Assuming both q_f and q_b are far smaller than Λ_q, one can set $\Lambda_q \to \infty$. Momentum integration then can be done explicitly, and the result is

$$\Sigma^{\rm th}(\omega_m) = \frac{g^* T}{4 m v_F} \mathrm{sgn}(\omega_m) \equiv \pi T \left(\frac{\bar{g}}{M}\right)^{1/3} \mathrm{sgn}(\omega_m), \tag{A10}$$

where

$$M = \frac{64}{3^{9/2}} \frac{m^3}{\alpha}. \tag{A11}$$

The total self-energy $\Sigma(k) = \Sigma^{\rm th}(k) + \Sigma^q(k)$ is

$$\Sigma(\omega_m) \simeq \left[\pi T \left(\frac{\bar{g}}{M}\right)^{1/3} + \frac{3}{2} \bar{g}^{1/3} |\omega_m|^{2/3}\right] \mathrm{sgn}(\omega_m). \tag{A12}$$

The two terms become comparable at

$$\omega_{\rm cross}(T) \sim \frac{T^{3/2}}{M^{1/2}}. \tag{A13}$$

Thermal self-energy is larger at $\omega_m < \omega_{\rm cross}(T)$.

Equation (A12) is valid when $q_f^{\rm typ} \ll q_b^{\rm typ}$, i.e., when

$$\tilde{\Sigma}(\omega_m)/v_F \ll m. \tag{A14}$$

At $\omega_m < \omega_{\rm cross}$, $\Sigma^{\rm th} > \Sigma^q$, and Eq. (A14) sets the condition on temperature

$$M < T < T^* \sim \bar{g} \left(\frac{M}{\bar{g}}\right)^{2/3} \left(\frac{E_F}{\bar{g}}\right)^{1/2}. \tag{A15}$$

At $\omega_m > \omega_{\rm cross}$, $\Sigma^{\rm th} < \Sigma^q$, and Eq. (A14) sets the condition on frequency

$$\omega_{\rm cross} < \omega_m < \omega^* \sim \bar{g} \left(\frac{M}{\bar{g}}\right)^{1/2} \left(\frac{E_F}{\bar{g}}\right)^{3/4}. \tag{A16}$$

One can check that self-consistency condition $\omega^* > \omega_{\rm cross}$ leads to the same condition on T as Eq. (A15). Then, when Eq. (A15) is satisfied, factorization of momentum integration is valid for all frequencies up to ω^*. We illustrate this in Fig. 9.

We emphasize that the T range in Eq. (A15) does exists at small but finite M simply because $M^{2/3} > M$, but collapses at a QCP, where $M = 0$. In other words, factorization of momentum integration in the integral for $\Sigma^{\rm th}$ holds only away from a QCP.

There is one more condition. We assumed above that $\Sigma_k \gg \omega_m$. A simple analysis shows that this condition is satisfied at arbitrary ratio of $\Sigma^{\rm th}$ and Σ^q when $M < \bar{g}^{5/2}/E_F^{3/2}$. This relation obviously holds for small M.

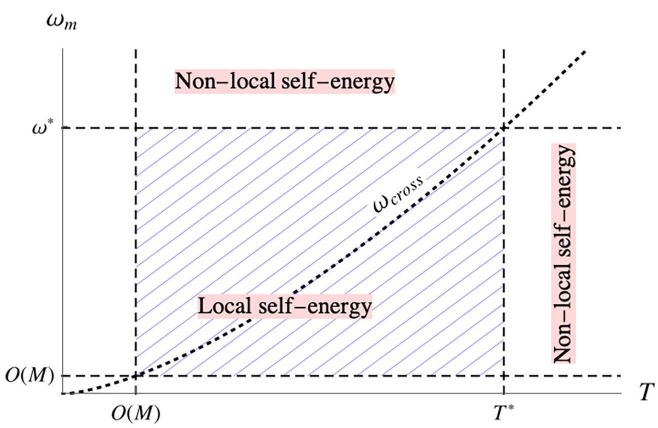

FIG. 9. Parameter range where the self-energy given by Eq. (A12) is local, i.e., momentum-independent (marked by "Local" in the plot).

3. Nonlocal self-energy

At temperatures above T^*, the condition $q_\parallel^{\text{typ}} \gg q_\perp^{\text{typ}}$ in the integral for Σ^{th} is not satisfied. The integration over $q_\parallel$ in Eq. (A5) can be done explicitly:

$$\int_{-\Lambda_q}^{\Lambda_q} \frac{dq_\parallel}{q_\parallel^2 + q_\perp^2 + m^2} \approx \frac{\pi}{\sqrt{q_\perp^2 + m^2}}. \tag{A17}$$

Then

$$i\Sigma^{\text{th}}(k) = -\frac{g^2 AT}{4\pi} \int_{-\Lambda_q}^{\Lambda_q} \frac{dq_\perp}{i\tilde{\Sigma}(\omega_m, \boldsymbol{k}+\boldsymbol{q}) - \epsilon_{\boldsymbol{k}} - v_F q_\perp} \times \frac{1}{\sqrt{q_\perp^2 + m^2}}. \tag{A18}$$

One can verify (see below) that at $T \gg T^*$, the leading term in this integral is obtained by ignoring the $\boldsymbol{q}$ dependence in the ferminonic propagator and pulling it out of the integral, i.e., by approximating

$$\int_{-\Lambda}^{\Lambda} \frac{dq_\perp}{i\tilde{\Sigma}(k+q) - \epsilon_{\boldsymbol{k}} - v_F q_\perp} \frac{1}{\sqrt{q_\perp^2 + m^2}} \simeq \frac{2\log\left(\frac{1}{m}\right)}{i\tilde{\Sigma}(k) - \epsilon_{\boldsymbol{k}}}. \tag{A19}$$

This leads to an algebraic relation

$$\Sigma^{\text{th}}(k) = \frac{B}{(\Sigma^{\text{th}}(k) + \tilde{\Sigma}^q(k)) + i\epsilon_{\boldsymbol{k}}}, \tag{A20}$$

where $\tilde{\Sigma}^q(k) = \Sigma^q(k) + \omega_m$, and

$$B = \frac{g^* T}{2\pi} \log\left(\frac{1}{m}\right). \tag{A21}$$

Equation (A20), viewed as quadratic equation on $\Sigma^{\text{th}}(k)$, has two solutions. The physical one must satisfy the boundary condition $\Sigma^{\text{th}} = 0$ at $B = 0$. This selects out the solution

$$\Sigma^{\text{th}}(k) = -\frac{\tilde{\Sigma}^q(\omega_n) + i\epsilon_{\boldsymbol{k}}}{2} + \text{sgn}(\omega_n)\sqrt{\frac{(\tilde{\Sigma}^q(\omega_n) + i\epsilon_{\boldsymbol{k}})^2}{4} + B}. \tag{A22}$$

We remind that we define $\sqrt{z}$ with a branch cut along the negative real axis of the complex variable z. One can verify that upon $\omega_m \leftrightarrow -\omega_m$ and $\epsilon_{\boldsymbol{k}} \leftrightarrow -\epsilon_{\boldsymbol{k}}$, $\Sigma^{\text{th}}(k)$ transforms as

$$\text{Re}\Sigma^{\text{th}}(\omega_m, \epsilon_{\boldsymbol{k}}) = -\text{Re}\Sigma^{\text{th}}(-\omega_m, \epsilon_{\boldsymbol{k}}) = +\text{Re}\Sigma^{\text{th}}(\omega_m, -\epsilon_{\boldsymbol{k}}), \tag{A23}$$

$$\text{Im}\Sigma^{\text{th}}(\omega_m, \epsilon_{\boldsymbol{k}}) = +\text{Im}\Sigma^{\text{th}}(-\omega_m, \epsilon_{\boldsymbol{k}}) = -\text{Im}\Sigma^{\text{th}}(\omega_m, -\epsilon_{\boldsymbol{k}}). \tag{A24}$$

When $\Sigma^{\text{th}}(k) > \tilde{\Sigma}^q$, $\Sigma^{\text{th}}(k) \approx \sqrt{B}\text{sgn}(\omega_n)$.

Equation (A22) has been obtained in Ref. [29] for $\epsilon_k = 0$. We will be chiefly interested in the consequences of the dependence of $\Sigma^{\text{th}}(k)$ on ϵ_k.

The total self-energy is given by $\Sigma(k) = \Sigma^{\text{th}}(k) + \Sigma^q(k)$, with the quantum part given by Eq. (A8). Expanding the self-energy to linear order in $\epsilon_{\boldsymbol{k}}$ we find

$$\Sigma(\omega_m, \epsilon_{\boldsymbol{k}}) \simeq \Sigma(\omega_m, 0) - \frac{i}{2}\left(1 - \frac{|\Sigma^q(\omega_m)|}{\sqrt{[\Sigma^q(\omega_m)]^2 + 4B}}\right)\epsilon_{\boldsymbol{k}}, \tag{A25}$$

where

$$\Sigma(\omega_m, 0) = \frac{\tilde{\Sigma}^q(\omega_n)}{2} + \text{sgn}(\tilde{\Sigma}^q(\omega_n))\sqrt{\frac{1}{4}[\tilde{\Sigma}^q(\omega_n)]^2 + B}. \tag{A26}$$

The first term renormalizes the frequency dependence of the Green's function, while the second term renormalizes the Fermi velocity into

$$v_F^* = \frac{1}{2}\left(1 + \frac{|\Sigma^q(\omega_m)|}{\sqrt{[\Sigma^q(\omega_m)]^2 + 4B}}\right) v_F. \tag{A27}$$

The renormalized velocity becomes $v_F/2$ when $\Sigma^{\text{th}} > \tilde{\Sigma}^q$, i.e., when $2\sqrt{B} \gg \Sigma^q(\omega_m)$, and differs only slightly from v_F when $\Sigma^{\text{th}} < \tilde{\Sigma}^q$. The crossover between the two regimes is at frequency

$$\tilde{\omega}_{\text{cross}} \sim \frac{B^{3/4}}{\bar{g}^{1/2}} = \bar{g}\left(\frac{T}{\bar{g}}\right)^{3/4}\left(\frac{E_F}{\bar{g}}\right)^{3/8} \log^{3/4}\left(\frac{1}{m}\right). \tag{A28}$$

We next consider the applicability range for Eq. (A24). Let us set $\epsilon_k = 0$ to avoid unnecessary complications. In obtaining Eq. (A24) we assumed that

$$\tilde{\Sigma}_k / v_F > m. \tag{A29}$$

At $\omega_m \ll \tilde{\omega}_{\text{cross}}$, $|\Sigma_k| \approx |\Sigma^{\text{th}}| = \sqrt{B}$, and the inequality in Eq. (A29) sets the condition on T:

$$T > \bar{g}\left(\frac{M}{\bar{g}}\right)^{2/3}\left(\frac{E_F}{\bar{g}}\right)^{1/2} \frac{1}{\log(1/m)} \sim \frac{T^*}{\log 1/m}. \tag{A30}$$

Up to a logarithm, this is $T > T^*$, i.e., $T = T^*$ is a sharp boundary between local and nonlocal forms of Σ^{th}. Keeping the logarithm one obtains [29] an extended crossover regime. It formally becomes wide at $m \to 0$, but like we said, we assume that mode-mode coupling cuts $\log m$ at $\log T$. Then the crossover regime is rather narrow. The upper limit on T,

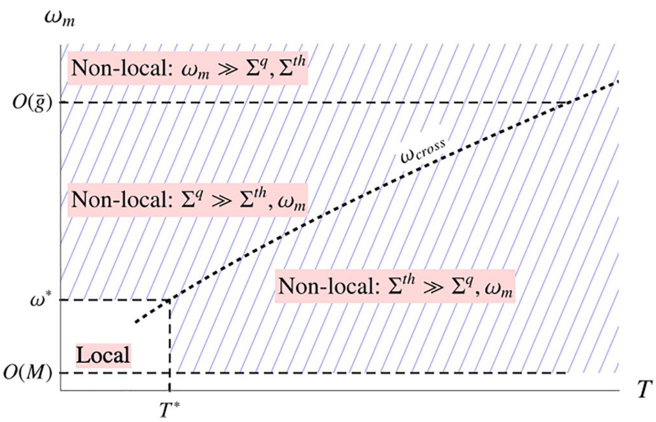

FIG. 10. Parameter range where the self-energy $\Sigma^{\rm th}(k)$ is nonlocal (marked by "Nonlocal" in the plot).

at which

$$T < T_{\rm max} \sim \bar{g}\left(\frac{E_F}{\bar{g}}\right)^{1/2} \tag{A31}$$

is set by the boundary condition on the momentum independence of the thermal self-energy.

At $\omega_m \ll \tilde{\omega}_{\rm cross}$, Eq. (A24) is valid in the same range of T, up to a frequency $\omega \sim \bar{g}$. We illustrate this in Fig. 10.

APPENDIX B: CANCELLATION OF $\Sigma^{\rm th}(k)$ IN THE FREE ENERGY

In this Appendix, we show explicitly that the thermal self-energy $\Sigma^{\rm th}$ cancels out in the free energy F_{el}, Eq. (3). This holds when $\Sigma^{\rm th}$ is local, and when it is nonlocal and given by Eq. (A24).

1. Case of local self-energy: $\Sigma(k) = \Sigma(\omega_n)$

When the self-energy is independent to $\epsilon_{\boldsymbol{k}}$, the momentum integration is straightforward,

$$\sum_{\boldsymbol{k}} \log\left(\frac{i\tilde{\Sigma}(\omega) - \epsilon_{\boldsymbol{k}}}{\epsilon_{\boldsymbol{k}}}\right) = N_F[\pi|\tilde{\Sigma}(\omega_n)| + i\pi\Lambda_q {\rm sgn}(\omega_n)], \tag{B1}$$

$$\sum_{\boldsymbol{k}} \frac{\Sigma(\omega)}{\tilde{\Sigma}(\omega) + i\epsilon_{\boldsymbol{k}}} = N_F\pi|\Sigma(\omega_n)|. \tag{B2}$$

Upon summation over ω_n we obtain

$$F_{el} = -2T\sum_{\omega_n} \pi N_F(|\tilde{\Sigma}(\omega_n)| - |\Sigma(\omega_n)|)$$
$$\equiv -2\pi T N_F \sum_{\omega_n} |\omega_n|, \tag{B3}$$

which is equal to the free energy of the noninteracting Fermi gas. The self-energy cancels out from this expression.

2. Case of nonlocal $\Sigma^{\rm th}(k)$

We now show that the cancellation holds even when $\Sigma^{\rm th}$ depends on the dispersion $\epsilon_{\boldsymbol{k}}$.

The electronic part of the free energy per volume is

$$F_{\rm el} = -T\sum_k \ln\left(\frac{(i\tilde{\Sigma}(k) - \epsilon_{\boldsymbol{k}})(i\tilde{\Sigma}(-k) - \epsilon_{-\boldsymbol{k}})}{\epsilon_{\boldsymbol{k}}^2}\right)$$
$$+ 2T\sum_k \frac{\tilde{\Sigma}(k) - \omega_m}{\tilde{\Sigma}(k) + i\epsilon_{\boldsymbol{k}}}. \tag{B4}$$

We show below that the nonlocal $\Sigma^{\rm th}(k)$ actually cancels out in each of two contributions to $F_{\rm el}$.

Substituting $\Sigma^{\rm th}$ from Eq. (A22) into the first term, we obtain after simple algebra

$$[i\tilde{\Sigma}(k) - \epsilon_{\boldsymbol{k}}][i\tilde{\Sigma}(-k) - \epsilon_{-\boldsymbol{k}}]$$
$$= \left(\frac{|\tilde{\Sigma}^q(\omega_m)| \pm i\epsilon_{\boldsymbol{k}}}{2} + \sqrt{\frac{(|\tilde{\Sigma}^q(\omega_m)| \pm i\epsilon_{\boldsymbol{k}})^2}{4} + B}\right)$$
$$\times \left(\frac{|\tilde{\Sigma}^q(\omega_m)| \pm i\epsilon_{\boldsymbol{k}}}{2} + \sqrt{\frac{(|\tilde{\Sigma}^q(\omega_m)| \pm i\epsilon_{\boldsymbol{k}})^2}{4} + B}\right), \tag{B5}$$

where $\pm$ refers to ${\rm sgn}(\omega_m)$. Introducing $|\tilde{\Sigma}^q(\omega_m)| = 2\sqrt{B}y$ and $\epsilon_{\boldsymbol{k}} = 2\sqrt{B}z$, we re-express Eq. (B5) as

$$\frac{[i\tilde{\Sigma}(k) - \epsilon_k][i\tilde{\Sigma}(-k) - \epsilon_{-\boldsymbol{k}}]}{\epsilon_{\boldsymbol{k}}^2}$$
$$= \frac{1}{4z^2}\left(y \pm iz + \sqrt{\frac{(y \pm iz)^2}{4} + B}\right)^2. \tag{B6}$$

To obtain the first term in $F_{\rm el}$, we need to integrate this expression over ϵ_k (i.e., over z) and sum up over Matsubara frequencies. Combining contribution from positive and negative z, we obtain

$$F_{el}^{(1)} = -T\sum_k \ln\left\{\frac{[i\tilde{\Sigma}(k) - \epsilon_{\boldsymbol{k}}][i\tilde{\Sigma}(-k) - \epsilon_{-\boldsymbol{k}}]}{\epsilon_{\boldsymbol{k}}^2}\right\}$$
$$= -4\sqrt{B}N_F T\sum_{\omega_m}\int_0^\Lambda dz \ln\left\{\frac{1}{4z^2}\left[y + iz + \sqrt{\frac{(y+iz)^2}{4} + B}\right]\left[y - iz + \sqrt{\frac{(y-iz)^2}{4} + B}\right]\right\}$$
$$= -4\pi\sqrt{B}N_F T\sum_{\omega_m} y = -2\pi N_F T\sum_{\omega_m}|\tilde{\Sigma}^q(\omega_m)|. \tag{B7}$$

We see that the result is the same as if $\Sigma^{\rm th}$ was absent.

For the second term in $F_{\rm el}$, we again use Eq. (A22) and express $\Sigma^{\rm th}$ in terms of $\tilde{\Sigma}^q$ and ϵ_k. This yields

$$\frac{\tilde{\Sigma}(k)-\omega_m}{\tilde{\Sigma}(k)+i\epsilon_{\mathbf{k}}} = \frac{\frac{\tilde{\Sigma}^q(k)-i\epsilon_k}{2}+\sqrt{\frac{(\tilde{\Sigma}^q(k)+i\epsilon_k)^2}{4}+B\mathrm{sgn}(\omega_m)}-\omega_m}{\frac{\tilde{\Sigma}^q(k)-i\epsilon_k}{2}+\sqrt{\frac{(\tilde{\Sigma}^q(k)+i\epsilon_k)^2}{4}+B\mathrm{sgn}(\omega_m)}+i\epsilon_{\mathbf{k}}}. \tag{B8}$$

Re-expressing in terms of y and z, as before, we obtain

$$\begin{aligned}\sum_{\mathbf{k}}\frac{\tilde{\Sigma}(k)-\omega_m}{\tilde{\Sigma}(k)+i\epsilon_{\mathbf{k}}} &= 2\sqrt{B}N_F\int_{-\Lambda_q/(2\sqrt{B})}^{\Lambda_q/(2\sqrt{B})}dz\frac{y-iz+\sqrt{(y+iz)^2+1}}{y+iz+\sqrt{(y+iz)^2+1}}\\ &\quad -2|\omega_m|N_F\int_{-\Lambda_q/(2\sqrt{B})}^{\Lambda_q/(2\sqrt{B})}dz\frac{1}{y+iz+\sqrt{(y+iz)^2+1}}.\end{aligned} \tag{B9}$$

This integral is convergent with typical $z=O(1)$. Given that $\Lambda \gg \sqrt{B}$, the z integration can be extended to infinite limits. Integrating in infinite limits, we obtain

$$\int_{-\infty}^{\infty}dz\frac{y-iz+\sqrt{(y+iz)^2+1}}{y+iz+\sqrt{(y+iz)^2+1}} = y\int_{-\infty}^{\infty}dt\frac{1-it+\sqrt{(1+it)^2+y^{-2}}}{1+it+\sqrt{(1+it)^2+y^{-2}}}=\pi y, \tag{B10}$$

$$\int_{-\infty}^{\infty}dz\frac{1}{y+iz+\sqrt{(y+iz)^2+1}} = \int_{-\infty}^{\infty}dt\frac{1}{1+it+\sqrt{(1+it)^2+1}} \tag{B11}$$

$$=\pi/2. \tag{B12}$$

Collecting contributions, we find

$$F_{\rm el}^{(2)} = 2T\sum_k\frac{\tilde{\Sigma}(k)-\omega_m}{\tilde{\Sigma}(k)+i\epsilon_{\mathbf{k}}} = 2\pi TN_F(|\tilde{\Sigma}^q(\omega_m)|-|\omega_m|), \tag{B13}$$

as if $\Sigma^{\rm th}$ was absent. Combining $F_{\rm el}^{(1)}$ and $F_{\rm el}^{(2)}$, we obtain

$$F_{\rm el} = -2\pi TN_F\sum_{\omega_m}|\omega_m|, \tag{B14}$$

which is the free energy of a noninteracting Fermi gas. We see that the self-energy cancels out in $F_{\rm el}$ even when $\Sigma^{\rm th}$ depends on $\epsilon_{\mathbf{k}}$.

APPENDIX C: EVALUATION OF FREE ENERGY

1. γ model at $\gamma = 0^+$

In the purely electronic γ model, the free energy is $F_\gamma = F_{\rm el}+F_{\rm int}$. For a generic nonzero γ, the free energy has been evaluated in Ref. [38]. Here, we compute the free energy for the special case $\gamma \to 0^+$, relevant to the analysis of the antiferromagnetic QCP (see the main text). The case $\gamma \to 0^+$ requires special care as the interaction $V(\Omega_m) \propto \log \bar{g}/|\Omega_m|$ For the free energy, we have in this case $F_{0+} = F_{\rm free}+F_{0+,\rm int}$, where in the notations from the main text

$$F_{0+,\rm int} = \frac{3g^*}{8\pi^3 v_F^2\beta}S_{0+}, \tag{C1}$$

$\beta = 2v_xv_y/v_F^2$, and

$$S_{0+} = (2\pi T)^2\sum_{n,n'=-M_f}^{M_f-1}\mathrm{sgn}(2n+1)\mathrm{sgn}(2n'+1)\log\frac{|n-n'|2\pi T}{T_0^{**}}. \tag{C2}$$

The thermal contribution, from $n=n'$, has to be evaluated at a nonzero bosonic mass. This contribution to F_{0+} is linear in T and does not affect the specific heat. Summing over $n' \neq n$, we obtain

$$S_{0+} = 4(2\pi T)^2\left(2\sum_{n=1}^{M_f-1}\log(n!)-\frac{1}{2}\sum_{n=1}^{2M_f-1}\log(n!)\right) - 4\pi T\Lambda\log\frac{2\pi T}{T_0^{**}}. \tag{C3}$$

Contributions from $n \sim O(1)$ are of order $\sim T^2$. We show that the summation over $n \gg 1$ yields a larger $\sim T^2\log(T)$ term. To evaluate this contribution, we use the asymptotic formula

$$\log(n!) = \left(n+\frac{1}{2}\right)\log(n)-n+\frac{1}{2}\log(2\pi) + \frac{1}{12n}+O\left(\frac{1}{n^2}\right), \tag{C4}$$

Substituting into Eq. (C3) and using

$$\begin{aligned}\sum_{n=1}^{M_f-1}\left(n+\frac{1}{2}\right)\log(n) &= \frac{1}{2}M_f^2\log M_f - \frac{1}{4}M_f^2-\frac{1}{2}M_f+O(1),\\ \sum_{n=1}^{M_f-1}\frac{1}{n} &= \log(M_f)+O(1),\\ \sum_{n=1}^{M_f-1}n &= M_f^2/2-M_f/2,\\ \sum_{n=1}^{M_f-1}1 &= M_f-1,\end{aligned} \tag{C5}$$

and the relation between M_f and the upper theory cutoff Λ, we obtain

$$S_{0+} = 4(2\pi T)^2\left[-M_f^2\log 2 + \frac{1}{2}\log(2\pi)M_f - \frac{1}{8}\log M_f + O(1)\right] - 2(2\pi T)^2 M_f \log\left(\frac{T}{T_0^{**}}\right)$$
$$= -\Lambda^2\log(16) + 4\pi\Lambda T\log\left(\frac{T_0^{**}}{2\pi T}\right) - 2\pi^2T^2\log\left(\frac{\Lambda}{T}\right) + O(T^2). \tag{C6}$$

Hence,

$$F_{0+}^{\text{int}} = N_F\frac{3g^*}{2\pi^2\beta E_F}\left[-\Lambda^2\log(2) + \pi\Lambda T\log\left(\frac{T_0^{**}}{T}\right) - \frac{1}{2}\pi^2T^2\log\left(\frac{\Lambda}{T}\right) + O(T^2)\right]. \tag{C7}$$

Differentiating twice with respect to temperature, one obtains the specific heat

$$C_{0+}^{\text{int}}(T) = N_F\frac{3g^*}{2\pi\beta E_F}\left[\Lambda + \pi T\log\left(\frac{\Lambda}{T}\right) + O(T)\right]. \tag{C8}$$

It contains a constant $\propto \Lambda$ and a universal $T\log(1/T)$ term.

For comparison, we evaluate the free energy of the regularized γ model, $\bar{F}_{0+} = F_{\text{free}} + \bar{F}_{0+}^{\text{int}}$, where

$$\bar{F}_{0+}^{\text{int}} = \frac{3g^*}{8\pi^3 v_F^2\beta}\bar{S}_{0+}, \tag{C9}$$

and

$$\bar{S}_{0+} = (2\pi T)^2\sum_{n,n'=-M_f}^{M_f-1}[\text{sgn}(2n+1)\text{sgn}(2n'+1) - 1]\log\frac{|n-n'|2\pi T}{T_0^{**}}. \tag{C10}$$

Since the summand is nonzero only when $2n+1$ and $2n'+1$ has opposite signs, the thermal part with $n = n'$ is avoided. The sum is evaluated in the same way as for the original γ model, and the result gives rise to

$$\bar{S}_{0+} = 4(2\pi T)^2\left[2\sum_{n=0}^{M_f-1}\log(n!) - \sum_{n=0}^{2M_f-1}\log(n!)\right] - 4(2\pi T)^2M_f^2\log\frac{2\pi T}{T_0^{**}}$$
$$= 4(2\pi T)^2\left[-M_f^2\log M_f + \log\left(\frac{e^{3/2}}{4}\right)M_f^2 - \frac{1}{12}\log M_f + O(1)\right] - 4(2\pi T)^2M_f^2\log\frac{2\pi T}{T_0^{**}}$$
$$= 4\Lambda^2\log\frac{e^{3/2}T_0^{**}}{4\Lambda} - \frac{4}{3}\pi^2T^2\log\left(\frac{\Lambda^2}{2\pi T T_0^{**}}\right) + O(T^2). \tag{C11}$$

As expected, the cutoff-dependent $\Lambda T\log(1/T)$ term is removed. The coefficient of the universal $T^2\log(1/T)$ term is 2/3 of that in the original γ model. This is the same ratio as for a nonzero γ (see the main text). The interaction part of the free energy is

$$\bar{F}_{0+}^{\text{int}} = -N_F\frac{3g^*}{2\pi^2\beta E_F}\left[\Lambda^2\log\left(\frac{4\Lambda}{e^{3/2}T_0^{**}}\right) + \frac{1}{3}\pi^2T^2\log\left(\frac{\Lambda^2}{2\pi T T_0^{**}}\right) + O(T^2)\right]. \tag{C12}$$

Differentiating twice with respect to temperature, we obtain the specific heat

$$\bar{C}_{0+}^{\text{int}}(T) = N_F\frac{g^*}{\beta E_F}T\log\left(\frac{\Lambda^2}{2\pi T T_0^{**}}\right) + O(T). \tag{C13}$$

2. Boson-fermion model

The free energy of the underlying boson-fermion model is given by $F = F_{\text{free}} + F_{\text{bos}}$, where

$$F_{\text{bos}} = \frac{k}{2}T\sum_q \log\left(-D_q^{-1}\right), \tag{C14}$$

and k is the number of components of the bosonic fields: $k = 1$ for Ising-nematic and electron-phonon cases, and $k = 3$ for an antiferromagnetic QCP. We presented the results for F_{bos} for the three cases in the main text. Here we show the details of the evaluation of F_{bos}^*.

a. Ising-nematic QCP

Subtracting frequency-independent term from $\log(-D_q^{-1})$ and integrating over the momentum in Eq. (C14) we obtain

$$F_{\text{bos}} = \frac{T}{2}\sum_{\Omega_n}\int\frac{d^2\boldsymbol{q}}{4\pi^2}\log\left(1+\frac{\alpha|\Omega_n|}{q^3}\right) = \frac{\alpha^{2/3}}{4\sqrt{3}}T\sum_{\Omega_n}|\Omega_n|^{2/3}. \tag{C15}$$

The frequency sum over $2M_b + 1$ Matsubara frequencies is expressed via the Harmonic number $\sum_{n=1}^{M_b} n^{2/3} = H_{-2/3}(M_b)$. Then $F_{\text{bos}} = \alpha^{2/3}(2\pi T)^{5/3}H_{-2/3}(M_b)/4\sqrt{3}\pi$.

Using the expansion of Harmonic number at large argument, $H_{-2/3}(M_b) = (3/5)(M_b + 1/2)^{5/3} + \zeta(-2/3) + O(1/(M_b + 1/2)^{1/3})$, and using the relation between M_b and Λ, Eq. (32), we obtain

$$F_{\text{bos}} = \frac{\alpha^{2/3}}{4\sqrt{3}\pi}\left[\frac{3}{5}\Lambda^{5/3} + \zeta\left(-\frac{2}{3}\right)(2\pi T)^{5/3}\right]. \tag{C16}$$

Differentiating twice over temperature and combining with free-fermion contribution, we obtain $C_{I-N}(T)$, given by Eq. (35).

b. Antiferromagnetic QCP

For this case, the momentum integral in Eq. (C14) is logarithmically singular and depends on the upper momentum cutoff $\Lambda_q \sim k_F$. Integrating over q, we obtain

$$F_{\text{bos}} = \frac{3\alpha T}{8\pi}\sum_{\Omega_n}|\Omega_n|\log\frac{\Lambda_q^2}{\alpha|\Omega_n|} \equiv -\frac{3\alpha}{2}T^2\sum_{n=1}^{M_b} n\log\frac{nT}{T_0}, \tag{C17}$$

where $T_0 \sim \Lambda_q^2/\alpha$. The frequency sum over $2M_b + 1$ Matsubara frequencies is expressed in terms of the hyperfactorial function $H(x)$ as

$$\sum_{n=1}^{M_b} n\log\frac{nT}{T_0} = \log\left[H(M_b)\right] + \frac{M_b(M_b+1)}{2}\log\frac{T}{T_0}. \tag{C18}$$

At large $M_b \gg 1$, $\log[H(M_b)]$ is expanded as

$$\log\left[H(M_b)\right] = -\tfrac{1}{4}M_b^2 + \left[\tfrac{1}{12} + \tfrac{1}{2}M_b(M_b+1)\right] \times \log(M_b) + \mathcal{O}(1). \tag{C19}$$

Using the relation between M_b and Λ, Eq. (32), we obtain after simple algebra

$$(2\pi T)^2\sum_{n=1}^{M_b} n\log\frac{nT}{T_0} = -\frac{1}{4}\Lambda^2 + \frac{1}{2}\Lambda^2\log\frac{\Lambda}{2\pi T_0} + \frac{1}{3}\pi^2T^2\log\frac{T_0}{T} + \mathcal{O}(T^2). \tag{C20}$$

Hence,

$$F_{\text{bos}} = -\frac{3\alpha}{16\pi^2}\Lambda^2\log\frac{\Lambda}{2\pi T_0\sqrt{e}} + \frac{\alpha}{8}T^2\log\frac{T}{T_0} + \mathcal{O}(T^2). \tag{C21}$$

c. QCP of an Einstein phonon

Near a QCP at which the dressed Debye frequency vanishes for $q < 2k - F$, the dressed phonon propagator takes the form $D_q^{-1} = \Omega_n^2 + \bar{\omega}_D^2 + 2\bar{g}^2|\Omega_n|/(v_F q)(2k_F/\sqrt{4k_F^2 - q^2})$, where ω_D and $\bar{\omega}_D = \omega_D(1-2\lambda)^{1/2}$ are bare and dressed Debye frequencies, and $\lambda = \bar{g}^2/\omega_D^2$. Substituting into Eq. (C14) and treating the Landau damping term as perturbation, we obtain

$$F_{\text{bos}} \simeq \frac{T}{2}\sum_{\Omega_n}\int\frac{d^2\boldsymbol{q}}{4\pi^2}\log\left(\Omega_n^2 + \bar{\omega}_D^2\right) + \frac{T}{2}\sum_{\Omega_n}\int\frac{d^2\boldsymbol{q}}{4\pi^2}\frac{2\bar{g}^2}{v_F q}\frac{|\Omega_n|}{\Omega_n^2 + \bar{\omega}_D^2}\frac{2k_F}{\sqrt{4k_F^2 - q^2}}, \tag{C22}$$

where the integration over q is up to $2k_F$. The first term is the free energy of a free Einstein phonon with the dressed Debye frequency $\bar{\omega}_D$:

$$F_{\text{bos}}^{(1)} = 4N_F E_F T\left[\log\bar{\omega}_D + 2\sum_{n=1}^{M_B}\log(2\pi T n) + \sum_{n=1}^{M_B}\log\left(1 + \frac{\bar{\omega}_D^2}{4\pi^2T^2n^2}\right)\right]. \tag{C23}$$

Using

$$\sum_1^{M_B}\log n = (M_b + 1/2)\log(M_b + 1/2)/e + \frac{1}{2}\log 2\pi,$$
$$\sum_1^{M_B}\log 2\pi T = (M_b + 1/2)\log 2\pi T - \frac{1}{2}\log 2\pi T, \tag{C24}$$

and the relation between M_B and Λ, we obtain

$$F_{\text{bos}}^{(1)} = 4N_F E_F\left[\frac{\Lambda}{\pi}\log\Lambda e + \sum_1^{M_B}\log\left(1 + \frac{\bar{\omega}_D^2}{4\pi^2T^2n^2}\right) - \log T\right]. \tag{C25}$$

The first term is T independent and does not contribute to entropy and specific heat. In the second term, the sum over m converges and the summation can be extended to $M_b = \infty$. Evaluating the sum using Euler-Maclauren formula and combining with the last term, we obtain

$$F_{\text{bos}}^{(1)} = 4N_F E_F\left[\frac{\Lambda}{\pi}\log\left(\frac{\Lambda}{e}\right) + T\log(1 - e^{-\bar{\omega}_D/T})\right]. \tag{C26}$$

We note in passing that the exponential temperature dependence of $F_{\text{bos}}^{(1)}$ at the smallest T implies that all terms in Euler-Maclauren series expansion in $T/\bar{\omega}_D$ vanish, as we explicitly verified.

Carrying out the momentum integration in the second term in Eq. (C22), we obtain

$$F_{\text{bos}}^{(2)} = \pi\bar{g}^2N_F T\sum_{\Omega_n}\frac{|\Omega_n|}{\Omega_n^2 + \bar{\omega}_D^2} = \bar{g}^2N_F\sum_{n=1}^{M_b}\frac{n}{n^2 + \left(\frac{\bar{\omega}_D}{2\pi T}\right)^2}. \tag{C27}$$

The sum over Matsubara frequencies is expressed via di-Γ functions as

$$\sum_{n=1}^{M_b}\frac{n}{n^2 + \left(\frac{\bar{\omega}_D}{2\pi T}\right)^2} = \text{Re}\left[\psi\left(1 + i\frac{\bar{\omega}_D}{2\pi T} + M_b\right) - \psi\left(1 + i\frac{\bar{\omega}_D}{2\pi T}\right)\right]. \tag{C28}$$

Using the asymptotic expression $\psi(z) \simeq \log(z)$ at $|z| \gg 1$ and re-expressing $\log \Lambda/(2\pi T)$ as $\log \Lambda/\bar{\omega}_D + \log \bar{\omega}_D/(2\pi T)$ we obtain

$$F_{\rm bos} = N_F\left[4E_F\frac{\Lambda}{\pi}\log\left(\frac{\Lambda}{e}\right) + \bar{g}^2\log\left(\frac{\Lambda}{\bar{\omega}_D}\right)\right] + 4N_F E_F T\left[\log\left(1-e^{-\bar{\omega}_D/T}\right) + \lambda_E\frac{\bar{\omega}_D}{4T}f\left(\frac{\bar{\omega}_D}{2\pi T}\right)\right], \tag{C29}$$

where the dimensionless function $f(x)$ is

$$f(x) = \log x - \tfrac{1}{2}\psi(1+ix) - \tfrac{1}{2}\psi(1-ix). \tag{C30}$$

This is Eq. (65) in the main text.

APPENDIX D: PHENOMENOLOGICAL MODELS THAT MAP TO THE γ-MODEL WITH $0 < \gamma < 1$

In this Appendix, we consider a phenomenological extension of the Ising-nematic model, which maps to the γ model with $\gamma = 1/3$, to a family of boson-fermion models that map to the γ-model with $0 < \gamma < 1$. The boson propagator takes the form

$$D_q^{-1} = -\left(q^{2-a} + \frac{\alpha|\Omega|}{q}\right)/D_0, \tag{D1}$$

where the parameter a is tunable. We assume that the Fermi surface is circular, like in the Ising-nematic case.

To establish the relation with the γ model, we compute the free energy, $F = F_{\rm el} + F_{\rm int}$. As in the Ising-nematic case, it can be re-expressed as $F = F_{\rm free} + F_{\rm int}$, where $F_{\rm free}$ is the contribution of free Fermi gas, and $F_{\rm int}$ comes from fermion-boson interaction

$$F_{\rm int} = -g^2T^2\sum_{m,m'}\int\frac{d^2\boldsymbol{k}d^2\boldsymbol{k}'}{(4\pi^2)^2}\frac{1}{i\tilde{\Sigma}(\omega_m)-\epsilon_{\boldsymbol{k}}} \times \frac{1}{i\tilde{\Sigma}(\omega'_m)-\epsilon_{\boldsymbol{k}'}}D_q, \tag{D2}$$

where $\boldsymbol{q} = \boldsymbol{k} - \boldsymbol{k}'$ by momentum conservation. We assume and then verify that typical momentum scale in the boson propagator, $\sim\omega^{1/(3-a)}$, is much larger than the one in the fermion propagator, $\sim\tilde{\Sigma}(\omega)/v_F$. In this situation, the momentum integration can be factorized as

$$F_{\rm int} = g^*T^2\sum_{m,m'}\int\frac{dk_\perp}{2\pi}\frac{1}{i\tilde{\Sigma}(\omega_m)-v_Fk_\perp}\int\frac{dk'_\perp}{2\pi} \times \frac{1}{i\tilde{\Sigma}(\omega'_m)-v_Fk'_\perp}\int\frac{dq_\parallel}{2\pi}\frac{1}{|q_\parallel|^{2-a}+\frac{\alpha|\omega_m-\omega'_m|}{|q_\parallel|}}. \tag{D3}$$

Carrying out the momentum integration, we obtain

$$F_{\rm int} = -\pi^2T^2N_F\bar{g}^{\frac{1-a}{3-a}}\sum_{m,m'}\sum_{\boldsymbol{k}\boldsymbol{k}'}\frac{{\rm sgn}(\omega_m\omega_{m'})}{|\omega_m-\omega_{m'}|^{\frac{1-a}{3-a}}}. \tag{D4}$$

This is equivalent to the free energy of the γ model with $\gamma = (1-a)/(3-a)$ and the effective coupling constant

$$\bar{g} = \left[\frac{1}{(3-a)\sin\frac{2\pi}{3-a}}\frac{g^*}{2\pi v_F\alpha^{\frac{1-a}{3-a}}}\right]^{\frac{3-a}{1-a}}. \tag{D5}$$

The effective γ changes continuously from 0 to 1 when a is changes between 1 to $-\infty$. For all these a, the coupling constant $\bar{g}^\gamma$ remains positive-defined. The sum in Eq. (D4) has been evaluated in the main text. It contains Λ-dependent terms and the universal term of order $T^{(5-a)/(3-a)}$. In the regularized γ model, Λ-dependent terms cancel out. The free energy is

$$\bar{F}_\gamma = F_{\rm free} + \frac{2}{4(3-a)\sin\frac{2\pi}{3-a}}\zeta\left(-\frac{2}{3-a}\right)(2\pi\alpha)^{\frac{2}{3-a}}T^{\frac{5-a}{3-a}}. \tag{D6}$$

The full free energy of the model includes the contribution from bosons,

$$F_{\rm full} = F_{\rm full}(T=0) - \frac{\pi^2}{3}N_FT^2 + \frac{1}{4\sin\frac{2\pi}{3-a}}\zeta\left(-\frac{2}{3-a}\right) \times (2\pi\alpha)^{\frac{2}{3-a}}T^{\frac{5-a}{3-a}}, \tag{D7}$$

where $F_{\rm full}(T=0)$ comes from the zero-temperature quantum fluctuations and depends on cutoff Λ. Comparing the T-dependent terms in $F_{\rm full}$ and $\bar{F}_\gamma$, we see that they have the same form, but the prefactors for the $T^{(5-a)/(3-a)}$ term differ by $2/(3-a)$. The prefactors agree at $a = 1+0$, when $\gamma = 0+$, as we also found in the explicit analysis of the $\gamma = 0+$ model in the main text.

[1] C. Nayak and F. Wilczek, Non-Fermi liquid fixed point in 2 + 1 dimensions, Nucl. Phys. B **417**, 359 (1994).

[2] S. Sachdev, A. V. Chubukov, and A. Sokol, Crossover and scaling in a nearly antiferromagnetic Fermi liquid in two dimensions, Phys. Rev. B **51**, 14874 (1995).

[3] A. J. Millis, Nearly antiferromagnetic Fermi liquids: An analytic Eliashberg approach, Phys. Rev. B **45**, 13047 (1992).

[4] A. Abanov, A. V. Chubukov, and J. Schmalian, Quantum-critical theory of the spin-Fermion model and its application to cuprates: Normal state analysis, Adv. Phys. **52**, 119 (2003).

[5] A. Abanov, A. V. Chubukov, and J. Schmalian, Fingerprints of spin mediated pairing in cuprates, J. Electron Spectrosc. Relat. Phenom. **117**, 129 (2001).

[6] D. J. Scalapino, A common thread: The pairing interaction for unconventional superconductors, Rev. Mod. Phys. **84**, 1383 (2012).

[7] D. Bergeron, D. Chowdhury, M. Punk, S. Sachdev, and A. M. S. Tremblay, Breakdown of Fermi liquid behavior at the $(\pi,\pi) = 2k_F$ spin-density wave quantum-critical point: The case of electron-doped cuprates, Phys. Rev. B **86**, 155123 (2012).

[8] K. B. Efetov, Quantum criticality in two dimensions and marginal Fermi liquid, Phys. Rev. B **91**, 045110 (2015).

[9] A. M. Tsvelik, Ladder physics in the spin fermion model, Phys. Rev. B **95**, 201112(R) (2017).
[10] F. Marsiglio, Eliashberg theory: A short review, Ann. Phys. **417**, 168102 (2020).
[11] A. V. Chubukov, A. Abanov, Y. Wang, and Y.-M. Wu, The interplay between superconductivity and non-Fermi liquid at a quantum-critical point in a metal, Ann. Phys. **417**, 168142 (2020).
[12] A. V. Chubukov, A. Abanov, I. Esterlis, and S. A. Kivelson, Eliashberg theory of phonon-mediated superconductivity—When it is valid and how it breaks down, Ann. Phys. **417**, 168190 (2020).
[13] B. L. Altshuler, L. B. Ioffe, and A. J. Millis, Low-energy properties of fermions with singular interactions, Phys. Rev. B **50**, 14048 (1994).
[14] A. Abanov, A. V. Chubukov, and A. M. Finkel'stein, Coherent vs incoherent pairing in 2D systems near magnetic instability, Europhys. Lett. **54**, 488 (2001).
[15] V. Oganesyan, S. A. Kivelson, and E. Fradkin, Quantum theory of a nematic Fermi fluid, Phys. Rev. B **64**, 195109 (2001).
[16] W. Metzner, D. Rohe, and S. Andergassen, Soft Fermi Surfaces and Breakdown of Fermi-Liquid Behavior, Phys. Rev. Lett. **91**, 066402 (2003).
[17] J. Rech, C. Pépin, and A. V. Chubukov, Quantum critical behavior in itinerant electron systems: Eliashberg theory and instability of a ferromagnetic quantum critical point, Phys. Rev. B **74**, 195126 (2006); A. V. Chubukov, C. Pépin, and J. Rech, Instability of the Quantum-Critical Point of Itinerant Ferromagnets, Phys. Rev. Lett. **92**, 147003 (2004).
[18] K. B. Efetov, H. Meier, and C. Pepin, Pseudogap state near a quantum critical point, Nat. Phys. **9**, 442 (2013).
[19] S. Raghu, G. Torroba, and H. Wang, Metallic quantum critical points with finite BCS couplings, Phys. Rev. B **92**, 205104 (2015); H. Wang, S. Raghu, and G. Torroba, Non-Fermi-liquid superconductivity: Eliashberg approach versus the renormalization group, *ibid.* **95**, 165137 (2017); H. Wang, Y. Wang, and G. Torroba, Superconductivity versus quantum criticality: Effects of thermal fluctuations, *ibid.* **97**, 054502 (2018); A. L. Fitzpatrick, S. Kachru, J. Kaplan, S. Raghu, G. Torroba, and H. Wang, Enhanced pairing of quantum critical metals near $d = 3 + 1$, *ibid.* **92**, 045118 (2015).
[20] S.-S. Lee, Low-energy effective theory of Fermi surface coupled with $U(1)$ gauge field in $2 + 1$ dimensions, Phys. Rev. B **80**, 165102 (2009); D. Dalidovich and S.-S. Lee, Perturbative non-Fermi liquids from dimensional regularization, *ibid.* **88**, 245106 (2013); A. Schlief, P. Lunts, and S.-S. Lee, Exact Critical Exponents for the Antiferromagnetic Quantum Critical Metal in Two Dimensions, Phys. Rev. X **7**, 021010 (2017).
[21] I. Mandal, Scaling behaviour and superconducting instability in anisotropic non-Fermi liquids, Ann. Phys. **376**, 89 (2017).
[22] N. E. Bonesteel, I. A. McDonald, and C. Nayak, Gauge Fields and Pairing in Double-Layer Composite Fermion Metals, Phys. Rev. Lett. **77**, 3009 (1996).
[23] L. Dell'Anna and W. Metzner, Fermi surface fluctuations and single electron excitations near pomeranchuk instability in two dimensions, Phys. Rev. B **73**, 045127 (2006); H. Yamase and W. Metzner, Fermi-Surface Truncation from Thermal Nematic Fluctuations, Phys. Rev. Lett. **108**, 186405 (2012).
[24] D. T. Son, Superconductivity by long-range color magnetic interaction in high-density quark matter, Phys. Rev. D **59**, 094019 (1999).
[25] A. V. Chubukov and J. Schmalian, Superconductivity due to massless boson exchange in the strong-coupling limit, Phys. Rev. B **72**, 174520 (2005).
[26] M. A. Metlitski and S. Sachdev, Quantum phase transitions of metals in two spatial dimensions. II. Spin density wave order, Phys. Rev. B **82**, 075128 (2010).
[27] D. F. Mross, J. McGreevy, H. Liu, and T. Senthil, Controlled expansion for certain non-Fermi-liquid metals, Phys. Rev. B **82**, 045121 (2010).
[28] A. V. Chubukov and P. Wölfle, Quasiparticle interaction function in a two-dimensional Fermi liquid near an antiferromagnetic critical point, Phys. Rev. B **89**, 045108 (2014).
[29] A. Klein, A. V. Chubukov, Y. Schattner, and E. Berg, Normal State Properties of Quantum Critical Metals at Finite Temperature, Phys. Rev. X **10**, 031053 (2020).
[30] M. A. Metlitski, D. F. Mross, S. Sachdev, and T. Senthil, Cooper pairing in non-Fermi liquids, Phys. Rev. B **91**, 115111 (2015).
[31] M. Punk, Finite-temperature scaling close to Ising-nematic quantum critical points in two-dimensional metals, Phys. Rev. B **94**, 195113 (2016).
[32] D. L. Maslov and A. V. Chubukov, Fermi liquid near Pomeranchuk quantum criticality, Phys. Rev. B **81**, 045110 (2010).
[33] C. M. Varma, Colloquium: Linear in temperature resistivity and associated mysteries including high temperature superconductivity, Rev. Mod. Phys. **92**, 031001 (2020).
[34] J. A. Damia, M. Solís, and G. Torroba, How non-Fermi liquids cure their infrared divergences, Phys. Rev. B **102**, 045147 (2020); H. Wang and G. Torroba, Non-Fermi liquids at finite temperature: Normal-state and infrared singularities, *ibid.* **96**, 144508 (2017).
[35] Y. Wang, A. Abanov, B. L. Altshuler, E. A. Yuzbashyan, and A. V. Chubukov, Superconductivity Near a Quantum-Critical Point: The Special Role of the First Matsubara Frequency, Phys. Rev. Lett. **117**, 157001 (2016).
[36] S. Lederer, Y. Schattner, E. Berg, and S. A. Kivelson, Superconductivity and non-Fermi liquid behavior near a nematic quantum critical point, Proc. Natl. Acad. Sci. USA **114**, 4905 (2017).
[37] A. Abanov and A. V. Chubukov, Interplay between superconductivity and non-Fermi liquid at a quantum critical point in a metal. I. the γ model and its phase diagram at $T = 0$: The case $0 < \gamma < 1$, Phys. Rev. B **102**, 024524 (2020); Y.-M. Wu, A. Abanov, Y. Wang, and A. V. Chubukov, Interplay between superconductivity and non-Fermi liquid at a quantum critical point in a metal. II. the γ model at a finite T for $0 < \gamma < 1$, *ibid.* **102**, 024525 (2020); Y.-M. Wu, A. Abanov, and A. V. Chubukov, Interplay between superconductivity and non-Fermi liquid behavior at a quantum critical point in a metal. III. the γ model and its phase diagram across $\gamma = 1$, *ibid.* **102**, 094516 (2020); Y.-M. Wu, S.-S. Zhang, A. Abanov, and A. V. Chubukov, Interplay between superconductivity and non-Fermi liquid at a quantum critical point in a metal. IV. the γ model and its phase diagram at $1 < \gamma < 2$, *ibid.* **103**, 024522 (2021);

Interplay between superconductivity and non-Fermi liquid behavior at a quantum-critical point in a metal. V. The γ model and its phase diagram: The case $\gamma = 2$, **103**, 184508 (2021); S.-S. Zhang, Y.-M. Wu, A. Abanov, and A. V. Chubukov, Interplay between superconductivity and non-Fermi liquid at a quantum critical point in a metal. vi. the γ model and its phase diagram at $2\gamma < 3$, *ibid.* **104**, 144509 (2021); Y.-M. Wu, S.-S. Zhang, A. Abanov, and A. V. Chubukov, Odd frequency pairing in a quantum critical metal, *ibid.* **106**, 094506 (2022).

[38] S.-S. Zhang, Y.-M. Wu, A. Abanov, and A. V. Chubukov, Superconductivity out of a non-Fermi liquid: Free energy analysis, Phys. Rev. B **106**, 144513 (2022).

[39] M. Protter, R. Boyack, and F. Marsiglio, Functional-integral approach to Gaussian fluctuations in Eliashberg theory, Phys. Rev. B **104**, 014513 (2021).

[40] E. A. Yuzbashyan and B. L. Altshuler, Migdal-Eliashberg theory as a classical spin chain, Phys. Rev. B **106**, 014512 (2022).

[41] E. A. Yuzbashyan and B. L. Altshuler, Breakdown of the Migdal-Eliashberg theory and a theory of lattice-fermionic superfluidity, Phys. Rev. B **106**, 054518 (2022).

[42] E. A. Yuzbashyan, Michael K.-H. Kiessling, and B. L. Altshuler, Superconductivity near a quantum critical point in the extreme retardation regime, Phys. Rev. B **106**, 064502 (2022).

[43] O. Grossman, J. S. Hofmann, T. Holder, and E. Berg, Specific Heat of a Quantum Critical Metal, Phys. Rev. Lett. **127**, 017601 (2021).

[44] E.-G. Moon and A. Chubukov, Quantum-critical pairing with varying exponents, J. Low Temp. Phys. **161**, 263 (2010).

[45] J. M. Luttinger and J. C. Ward, Ground-state energy of a many-fermion system. II, Phys. Rev. **118**, 1417 (1960).

[46] G. M. Eliashberg, Interactions between electrons and lattice vibrations in a superconductor, Sov. Phys. JETP **11**, 696 (1960) [Zh. Eksperim. i Teor. Fiz. **38**, 966 (1960)].

[47] J. Bardeen and M. Stephen, Free-energy difference between normal and superconducting states, Phys. Rev. **136**, A1485 (1964).

[48] R. E. Prange and L. P. Kadanoff, Transport theory for electron-phonon interactions in metals, Phys. Rev. **134**, A566 (1964).

[49] R. Haslinger and A. V. Chubukov, Condensation energy in strongly coupled superconductors, Phys. Rev. B **68**, 214508 (2003).

[50] A. V. Chubukov, D. L. Maslov, S. Gangadharaiah, and L. I. Glazman, Thermodynamics of a Fermi Liquid Beyond the Low-Energy Limit, Phys. Rev. Lett. **95**, 026402 (2005); Singular perturbation theory for interacting fermions in two dimensions, Phys. Rev. B **71**, 205112 (2005).

[51] A. Secchi, M. Polini, and M. I. Katsnelson, Phonon-mediated superconductivity in strongly correlated electron systems: A Luttinger–Ward functional approach, Ann. Phys. **417**, 168100 (2020).

[52] A. Benlagra, K. Kim, and C. Pépin, The Luttinger–Ward functional approach in the Eliashberg framework: A systematic derivation of scaling for thermodynamics near the quantum critical point, J. Phys.: Condens. Matter **23**, 145601 (2011).

[53] D. L. Maslov and A. V. Chubukov, Nonanalytic paramagnetic response of itinerant fermions away and near a ferromagnetic quantum phase transition, Phys. Rev. B **79**, 075112 (2009).

[54] D. Chowdhury and E. Berg, Intrinsic superconducting instabilities of a solvable model for an incoherent metal, Phys. Rev. Res. **2**, 013301 (2020).

[55] I. Esterlis, H. Guo, A. A. Patel, and S. Sachdev, Large-n theory of critical Fermi surfaces, Phys. Rev. B **103**, 235129 (2021).

[56] H. Guo, A. A. Patel, I. Esterlis, and S. Sachdev, Large-n theory of critical Fermi surfaces. II. Conductivity, Phys. Rev. B **106**, 115151 (2022).

[57] We assume, as in previous works on metallic QCP, that fermionic bandwidth W is the largest scale of the problem, and neglect terms, which are small in g/W.

[58] A. J. Millis, Effect of a nonzero temperature on quantum critical points in itinerant fermion systems, Phys. Rev. B **48**, 7183 (1993).

[59] J.-P. Blaizot and E. Iancu, Lifetimes of quasiparticles and collective excitations in hot qed plasmas, Phys. Rev. D **55**, 973 (1997).

[60] M. A. Metlitski and S. Sachdev, Quantum phase transitions of metals in two spatial dimensions. I. Ising-nematic order, Phys. Rev. B **82**, 075127 (2010).

[61] T. Holder and W. Metzner, Fermion loops and improved power-counting in two-dimensional critical metals with singular forward scattering, Phys. Rev. B **92**, 245128 (2015).

[62] A. Eberlein, I. Mandal, and S. Sachdev, Hyperscaling violation at the Ising-nematic quantum critical point in two-dimensional metals, Phys. Rev. B **94**, 045133 (2016).

[63] D. Pimenov, A. Kamenev, and A. V. Chubukov, One-dimensional scattering of two-dimensional fermions near quantum criticality, Phys. Rev. B **103**, 214519 (2021).

[64] J. A. Damia, S. Kachru, S. Raghu, and G. Torroba, Two-Dimensional Non-Fermi-Liquid Metals: A Solvable Large-n limit, Phys. Rev. Lett. **123**, 096402 (2019).

[65] M. Ye and A. V. Chubukov, Hubbard model on a triangular lattice: Pseudogap due to spin density wave fluctuations, Phys. Rev. B **100**, 035135 (2019).

[66] Y. Wang and A. V. Chubukov, Superconductivity at the Onset of Spin-Density-Wave Order in a Metal, Phys. Rev. Lett. **110**, 127001 (2013).

[67] A. L. Fitzpatrick, S. Kachru, J. Kaplan, and S. Raghu, Non-Fermi-liquid fixed point in a Wilsonian theory of quantum critical metals, Phys. Rev. B **88**, 125116 (2013).

[68] A. V. Chubukov and A. Abanov, Pairing by a dynamical interaction in a metal, J. Exp. Theor. Phys. **132**, 606 (2021).

[69] D. L. Maslov, P. Sharma, D. Torbunov, and A. V. Chubukov, Gradient terms in quantum-critical theories of itinerant fermions, Phys. Rev. B **96**, 085137 (2017).

[70] C. Zhang, J. Sous, D. R. Reichman, M. Berciu, A. J. Millis, N. V. Prokof'ev, and B. V. Svistunov, Bipolaronic High-Temperature Superconductivity, Phys. Rev. X **13**, 011010 (2023).

[71] A. V. Chubukov, Kohn-Luttinger effect and the instability of a two-dimensional repulsive Fermi liquid at $t = 0$, Phys. Rev. B **48**, 1097 (1993).

[72] I. Esterlis, B. Nosarzewski, E. W. Huang, B. Moritz, T. P. Devereaux, D. J. Scalapino, and S. A. Kivelson, Breakdown of the Migdal-Eliashberg theory: A determinant quantum Monte Carlo study, Phys. Rev. B **97**, 140501(R) (2018).

[73] R. Combescot, Strong-coupling limit of Eliashberg theory, Phys. Rev. B **51**, 11625 (1995).

[74] F. Marsiglio and J. P. Carbotte, Gap function and density of states in the strong-coupling limit for an electron-boson system, Phys. Rev. B **43**, 5355 (1991); for more recent results see F. Marsiglio and J. P. Carbotte, Electron-Phonon Superconductivity, in *The Physics of Conventional and Unconventional Superconductors*, edited by Bennemann and Ketterson (Springer-Verlag, Berlin, 2006) and references therein.

[75] A. V. Chubukov, P. Monthoux, and D. K. Morr, Vertex corrections in antiferromagnetic spin-fluctuation theories, Phys. Rev. B **56**, 7789 (1997).